Natural Resources Canada | Ressources naturelles Canada

GEOLOGICAL SURVEY OF CANADA
OPEN FILE 8049

Determination of hydrocarbon generation and expulsion temperature of organic-rich Upper Ordovician shales from Hudson Bay and Foxe basins using modified hydrous pyrolysis, organic petrography, Rock-Eval analysis and organic solvent extraction

J. Reyes, C. Jiang, D. Lavoie, M. Milovic, R. Robinson, S. Zhang, D. Armstrong, and A. Mort

2016

GEOLOGICAL SURVEY OF
CANADA OPEN FILE 8049

Determination of hydrocarbon generation and expulsion temperature of organic-rich Upper Ordovician shales from Hudson Bay and Foxe basins using modified hydrous pyrolysis, organic petrography, Rock-Eval analysis and organic solvent extraction

J. Reyes[1], C. Jiang[1], D. Lavoie[2], M. Milovic[1], R. Robinson[1], S. Zhang[3], D. Armstrong[4], and A. Mort[1]

[1]Geological Survey of Canada, Calgary, AB T2L 2A7
[2]Geological Survey of Canada, Quebec City, QC G1K 9A9
[3]Canada-Nunavut Geoscience Centre, Iqaluit, NU X0A 0H0
[4]Ontario Geological Survey Sudbury, ON P3E 6B5

2016

doi:10.4095/299254

This publication is available for free download through GEOSCAN (http://geoscan.nrcan.gc.ca/).

Recommended citation

Reyes, J., Jiang, C., Lavoie, D., Milovic, M. Robinson, R., Zhang, S., Armstrong, D., and Mort, A. 2016. Determination of hydrocarbon generation and expulsion temperature of organic-rich Upper Ordovician shales from Hudson Bay and Foxe basins using modified hydrous pyrolysis, organic petrography, Rock-Eval and organic solvent extraction; Geological Survey of Canada, Open File 8049, 62 p. doi:10.4095/299254

Publications in this series have not been edited; they are released as submitted by the author.

Table of Contents

SUMMARY

Immature organic-rich Ordovician mudstone and limy shale source rocks were artificially matured using modified hydrous pyrolysis in an attempt to characterize the thermal maturation history and hydrocarbon generation scenario. The experimental hydrous pyrolysis temperature range of 310-350 ^{o}C for 72 hours corresponds to hydrocarbon generation (HCG) at laboratory timescales. The Rock-Eval (RE) results show that the T_{max} of the pyrolyzed samples increased from 413 ^{o}C to 450 ^{o}C after the last stage (350 ^{o}C) of hydrous pyrolysis. Solvent extraction and RE analysis of pyrolyzed rock chips indicates that T_{max} suppression is associated with the high amount of free hydrocarbons and soluble solid bitumen or extractable organic matter in the samples.

The estimated vitrinite reflectance equivalent values calculated from the measured T_{max} (0.67 to 1.03 $\%Ro_{eqv\text{-}ext}$), chitinozoan (0.68 to 1.1 $\%Ro_{eqv}$) and bitumen (0.75 to 1.08 $\%Ro_{eqv}$) reflectance are in excellent agreement and indicate that all artificially matured samples reached HCG at 310°C. Organic petrographic analysis of the pyrolyzed rock chips from hydrous pyrolysis shows that bituminite and other amorphous kerogen are the first macerals to thermally degrade, followed by prasinophyte alginite. Some of the pore spaces created by the thermally degraded amorphous kerogen and bituminite are partially filled by soluble heavy bitumen. The solubility of the solid bitumen and the amount of free hydrocarbons decreases, and the fluorescence intensity of liptinite macerals shifts from bright yellow to reddish orange with increasing pyrolysis temperature. Free hydrocarbons in fracture and intergranular pore spaces were also observed in the rock matrix after hydrous pyrolysis.

Peak hydrocarbon generation occurs between pyrolysis temperatures of 330 and 350 ^{o}C with measured T_{max} values of 439 to 455 ^{o}C after solvent extraction. The quantity of generated hydrocarbons ranges from 22.75 to 166.22 mg HC/g TOC. Comparisons of the calculated TRs of HI and S2 from unextracted and extracted pyrolyzed rock chips clearly indicate that the unextracted samples underestimate the residual hydrocarbon potential of the pyrolyzed source rocks. The underestimation appears to be higher during the formation of heavy oil and soluble bitumen, which declines exponentially as the pyrolysis temperature increases.

Comparative analysis of the geochemical data from the offshore wells from the Hudson Bay Basin and the results of this study suggest that the observed large T_{max} variation among the samples from the offshore wells cannot be attributed to T_{max} suppression associated with a high amount of soluble organic matter and labile hydrocarbons. Almost all of the RE parameters show no indication of in-situ oil generation and migration. Petrographically, none of these previously analyzed offshore Upper Ordovician formations showed any direct evidence of in-situ hydrocarbon generation and migration unlike those observed in the artificially matured samples. If indeed the measured and estimated T_{max} values (>435 ^{o}C) are the effective maximum and current burial temperatures of these organic rich formations, migrated solid bitumen and free hydrocarbon will be visible within the intergranular pore spaces of the rock matrix at this level of thermal maturity.

INTRODUCTION

Past and recent geochemical analyses of Upper Ordovician potential source rocks from the Hudson Bay and adjacent Foxe basins have documented some interesting but yet intriguing data (Macauley et al, 1990; Zhang, 2008, 2011; Lavoie et al., 2013, 2015a). These potential source rocks are rich in total organic carbon (TOC) up to 34%, have very high hydrogen indices (HI) and are either immature (onshore outcrop samples) or early mature (offshore well cuttings) based on their relatively low T_{max} values (Zhang, 2008; Lavoie et al., 2013). These source rocks are also characterized by the presence of biomarkers suggestive of a restrictive, hypersaline and evaporative depositional environment, which is also supported by the sedimentary record and the presence of interbedded platform evaporites (Lavoie et al., 2013). The thicknesses of the source rock intervals are highly variable, from a few metres on Southampton Island in the northern part of Hudson Bay (Zhang, 2008) to 10-12 metres on Baffin Island and northern Ontario (Macauley, 1987; Lavoie et al., 2013). The source rock organic matter is dominantly Type II sulphur-rich kerogen (Macauly et al., 1990). Perceived lack of maturity was one of the critical elements raised by the industry to terminate hydrocarbon exploration in the area in the early 1980's (Lavoie et al., 2015)

Other thermal indicators gathered during the Hudson Bay GEM-1 project raised some issues with the thermal maturation of the Upper Ordovician succession of the Hudson Bay basin. Reflectance of various difference macerals suggested that the source rocks from wells drilled in the central part of the Hudson Bay Basin (Bertrand and Malo, 2012) are in the oil window, and immature to early mature in northern Ontario (Reyes et al., 2011). However, Reyes et al., (2011) did not observe any direct evidence of oil generation in the source rocks. Preliminary analyses of apatite fission tracks suggested that the Upper Ordovician source rocks could have entered the oil window (Lavoie et al., 2013). Indirect evidence of a working petroleum system, at least locally, include the presence of bitumen, oil staining and oil in Upper Ordovician reefs, and lower Silurian and Middle Devonian platform carbonates (Heywood and Sanford, 1976; Lavoie et al., 2013, 2015; Eggie et al., 2014). RADARSAT image analyses have also identified 41 reflectance anomalies that could be natural oil slicks on seawater; and a number of these are repetitive over time (Decker et al., 2013; Lavoie et

al., 2015).

A detailed re-examination of the T_{max} data from the Upper Ordovician succession shows that the T_{max} values of the source rocks were invariably 3 to 5°C lower than the values of the adjacent non-source rock interval (Lavoie et al., 2013). It was thus suggested that T_{max} was suppressed because of high TOC and HI and that the source rocks have already reached oil window conditions and generated some significant volume of hydrocarbons (Lavoie et al., 2013, 2015).

Geological Setting

The Hudson Bay Basin is the largest intracratonic basin in North America. The succession consists mainly of Paleozoic strata, with a maximum preserved thickness of about 2500 m (Pinet et al., 2013). The Paleozoic succession includes Ordovician to Devonian shallow marine carbonates, reefs and shales with locally thick Devonian evaporites. In some parts of the basin, Paleozoic strata are unconformably overlain by a thin Mesozoic/Cenozoic cover of non-marine and marine strata. From 1973 to 1985, over 46,000 line-km of marine seismic reflection data were acquired and 5 offshore exploration wells drilled, mostly in the central part of the basin.

Seismic data indicate that syn-tectonic sedimentation occurred in Late Ordovician(?), Silurian and Early Devonian, with significant depocentre migration with time (Pinet et al., 2013). Biostratigraphic data, supported by the seismic evidence, indicate an irregular subsidence history including exhumation events marked by major unconformities. Available hydrocarbon system data were synthesized in five conventional petroleum plays with the Upper Ordovician organic matter rich shaley limestones as source rocks (Lavoie et al., 2013, 2015).

Proposed Study

The contradictory thermal maturity indicators and the absence of hydrocarbon shows that are directly linked to the Upper Ordovician formations make it difficult to fully

ascertain whether or not they reached the oil window. The goal of this experiment is to determine hydrocarbon generation and expulsion temperatures for the specific intervals in question, and improve understanding of their thermal maturation indices and phases of petroleum generation. To accomplish these objectives, artificial maturation of immature organic-rich Upper Ordovician source rocks has been carried out in the laboratory using hydrous pyrolysis. The data and information collected from the experiments can be compared to and applied to our current understanding of the burial history and hydrocarbon generation potential of these formations and the Hudson Bay and Foxe basins as a whole.

Artificial Maturation

Artificial maturation of organic rich source rocks has been practiced in the laboratory for several decades (Lewan et al., 1979; Seifert and Moldovan, 1980; Lewan, 1985; Lewan 1987; Lewan, 1993; Winters et al., 1983; Soldan et al., 1988; Peters et al., 1990; Moldovan et al., 1992; Behar et al., 1997; Souza et al., 2014; Spigolon et al., 2015). Artificial maturation of organic matter is accomplished by attempting to simulate in situ hydrocarbon generation, but at elevated temperatures to compensate for shorter laboratory timescales. This process provides significant information about the physicochemical changes that result in petroleum generation. One of the most widely used methods for simulating source rock maturation is closed system hydrous pyrolysis (Seifert and Moldovan, 1980; Lewan, 1985; Lewan 1993; Peters et al., 2005b; Souza et al., 2014; Spigolon et al., 2015). It can provide valuable information on thermal maturation of kerogen, phases and kinetics of petroleum generation, and primary hydrocarbon generation and migration (Lewan et al., 1979; Lewan, 1985; Lewan 1987; Winters et al., 1983; Soldan et al., 1988; Peters et al., 1990; Moldovan et al., 1992; Lewan, 1993; Behar et al., 1997; Spigolon et al., 2015). Studies have shown that closed system hydrous pyrolysis may provide a more accurate simulation of natural oil generation than other methodologies such as closed system anhydrous pyrolysis (Seifert and Moldovan, 1980; Lewan, 1993; Lewan, 1997; Lewan and Roy, 2011, Spigolon et al., 2015). The most important aspect of closed system hydrous pyrolysis is that the produced oil compositionally resembles oil generated deep in the subsurface (Peters et al., 1990; Noble et al., 1991; Moldovan et al., 1992; Spigolon et al., 2015).

SAMPLES AND METHODS

Samples

Four immature organic-rich, shaley mudstone/limestone outcrop samples were collected from the Upper Ordovician Boas River, Red Head Rapids, Amadjuak, and Akpatok formations (Figure 1) and used in the experiments (Reyes et al., 2011, Zhang, 2011; Lavoie et al., 2013, Lavoie et al., 2015). The shaley mudstone sample of the Boas River Formation is located south of the Hudson Bay Basin in the northern Ontario. The sample from the Red Head Rapids Formation sample location is located north of Southampton Island, southeast of the Foxe Basin. The sample of the Amadjuak Formation is positioned in the southern section of the Baffin Island in Nunavut. The sample of the Akpatok Formation is located on Akpatok Island in the Ungava Bay, northern Quebec.

Previous geochemical analysis indicated these samples were deposited in a reducing marine paleodepositional environment and have varying dispersed organic matter (DOM) content and composition (Zhang, 2011; Bertrand and Malo, 2012; Zhang, 2012; Lavoie et al., 2013; Lavoie et al., 2015). The Boas River Formation has TOC content in the range of 0.38 to 12.84% (Reyes et al., 2011). The Red Head Rapids Formation shales have the highest TOC (up to 34%) compared to the other formations (Zhang, 2011). The Amadjuak Formation has TOC content ranging between 0.18 and 13.95% (Zhang, 2012). The brown bituminous limestone from the Akpatok Formation has the lowest TOC (0.51 to 2.11%) compared to the other formations. Based on the HI and OI data from RE analyses these formations contain mostly Type II kerogen (Zhang, 2011; Reyes et al., 2011; Zhang, 2012; Lavoie et al., 2013; Lavoie et al., 2015). The most important differences among these formations with respect to the organic facies are the local abundance of qualifier organic facies like *Gloeocapsomorpha prisca* (G. prisca) and zooclast graptolite, chitinozoan, conodont and other calcareous microfossils (Zhang, 2011; Reyes et al., 2011; Bertrand and Malo (2012); Zhang, 2012; Lavoie et al., 2013).

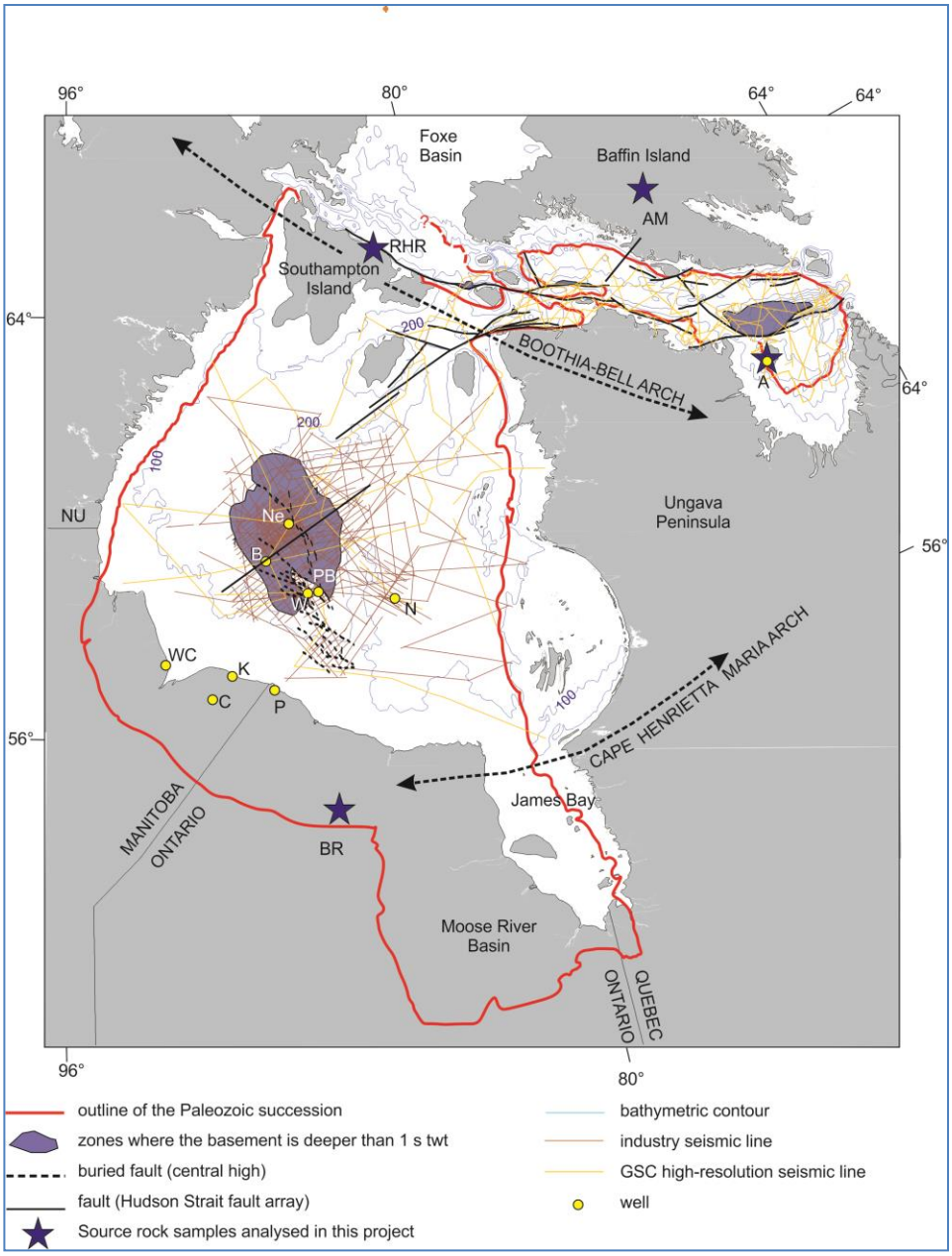

Figure 1. Map showing the extent of the Hudson Bay Basin and adjacent basins. Faults in the central Hudson Bay Basin (central high) are from Pinet et al. (2013a). Faults in the Hudson Strait are from Pinet et al. (2013b). Multichannel industry seismic lines and Geological Survey of Canada high-resolution seismic lines are depicted, with mapped areas where the seismically-imaged sedimentary succession is deeper than 1s two-way time. Bathymetric contour intervals are 100 m (330 ft). Exploration wells: A, Premium Homestead L-26 Akpatok; B, Trillium et al. O-23 Beluga; C, Houston et al. No.1 Comeault; K, Sogepet Aquitaine No.1 Kaskattama; N, Aquitaine et al. O-58 Narwhal South; Ne, ICG et al. N-01 Netsiq; P, Aquitaine No. 1 Pen Island; PB, Aquitaine et al. C-11 Polar Bear; W, Aquitaine et al. A-71 Walrus; WC, Merland Exploration No. 1 Whitebear Creek. BR is for Boas River Formation sample location; RHR is for Red Head Rapids Formation sample location; AM is for Amadjuak Formation sample location, and A for Akpatok Formation sample location. Modified from Lavoie et al. (2015).

Experimental Procedures

Rock samples were first crushed to 1 to 2 mm sizes to obtain homogenized laboratory samples for various analyses. Aliquots of the homogenized samples were then sent for petrographic and geochemical analyses to determine the baseline organic facies, thermal maturity and bulk geochemical properties of the original samples. Figure 2 shows a simplified diagram outlining the steps taken and analyses performed at every stage of the experiment. Organic petrography was carried out to determine the thermal maturity and organic facies of the dispersed organic matter. Rock-Eval analysis was performed on the original samples to determine the kerogen type, thermal maturity and oil generation potential of each formation. Aliquots of samples were sent for hydrous pyrolysis for artificial maturation of kerogen, which was completed in a standard gas chromatography (GC) oven.

After each stage of hydrous pyrolysis, the pyrolyzed rock chips were collected, dried and split into three aliquots to be sent for Rock-Eval analysis, organic petrology observation and organic solvent extraction. Aliquots of extracted pyrolyzed rock chips were also sent for Rock-Eval analysis for comparison with the corresponding unextracted samples. Oil collected from the pyrolysis vessels and the solvent extracts were sent for column chromatographic separation to separate the saturated, aromatic, resin and asphaltene (SARA) fractions. Whole extracts, saturated fractions and aromatic fractions obtained were analyzed by gas chromatography (GC), and gas chromatography-mass spectrometry (GC-MS) analysis. The results from GC and GC-MS analyses will be presented in a separate future report.

Organic Petrography

Organic petrography is the most commonly used analysis in the study of coal and coal combustion (Teichmüller, 1974; Mackowsky, 1982; Stach et al., 1982; Teichmüller 1987; Diessel and Bailey, 1989; Taylor et al., 1991; Potter et al., 1998; Stasiuk et al., 2005, Goodarzi et al., 2006), and has been applied to conventional and unconventional source rock evaluation (Stasiuk, 1993; Stasiuk, 1996; Stasiuk and Fowler, 2004; Reyes et al., 2011; Hackley et al. 2013), environmental studies (Reyes et al., 2006), and burial and

thermotectonic histories of sedimentary basins (Reyes et al., 2015a,b; Issler et al., 2012). In this study, organic petrography was used to qualitatively and quantitatively evaluate the physicochemical changes in kerogen composition within the source rocks after pyrolysis at various temperatures. To conform to accepted standards, the sample preparation followed Mackowsky (1982) "Methods and tools of examination" with minor modification to accommodate the samples being studied. ASTM D7708-11 "Standard test method for microscopical determination of the reflectance of vitrinite dispersed in sedimentary rocks" was also referred to in this study. Additionally, Jacob (1989) "Classification, structure, genesis and practical importance of natural solid oil bitumen ("migrabitumen")" was also used as guidance to characterize the solid bitumen in-situ after each stage of pyrolysis.

For petrographic observation, crushed whole rock samples were mounted in a one inch plastic mold using two part resin to form solid pellets. These pellets were then polished using five types of grinding and polishing materials with the addition of 0.5 and 0.03 alumina silica emulsions. Random reflectance measurements were carried out on bitumen and chitinozoan using Zeiss Axioplan microscope equipped with Fossil System for reflectance measurements. The microscope was calibrated before each analysis using precision yttrium-aluminum-garnet standards with a refractive index of 0.906 %Ro under oil immersion. Random reflectance measurements were performed on all the samples following ASTM D7708-11. Whenever possible, a minimum of 50 random reflectance measurements were done for each sample. In some cases, only limited numbers of reflectance measurements were made due to the limited quantity of the disseminated kerogen.

In the absence of true vitrinite macerals in the Upper Ordovician formations, bitumen and chitinozoan reflectance were used to estimate the vitrinite reflectance equivalent (VR_{eqv}). Chitinozoans are Paleozoic microfossils that are important stratigraphic biomarkers (Jenkins, 1970; Lipps, 1993). Migrated solid bitumen is the secondary product of the thermal decomposition of insoluble reactive kerogen in organic-rich rocks during late stage diagenesis and into catagenesis (Hunt, 1979; Curiale, 1986; Jacob, 1989; ICCP, 1993). There are several equations (Jacob, 1989, 1993; Bertrand, 1993; Landis and Castaño, 1995) that are used to correlate bitumen and vitrinite reflectance. Likewise, there are correlation equations to estimate VR_{eqv} from measured chitinozoan reflectance as well (Bertrand, 1990; Tricker et al., 1992; Obermajer et al., 1996). Petersen et al. (2013) and more recently

Hackley and Cardott (2016) provided a complete summary of the most commonly used correlation equations used to estimate vitrinite reflectance equivalent.

Rock-Eval Analysis

Rock-Eval analysis is a well-accepted and cost-efficient geochemical analysis used for oil and gas exploration (Tissot and Welte, 1984; Lewan, 1985; Peters, 1986; Bordenave et al., 1993; Peters and Cassa, 1994; Lafargue et al., 1998; Peters et al., 2005a; McCarthy et al., 2011; Spigolon et al., 2015, and references therein). However, it requires a comprehensive understanding of its capabilities and limitations in order to provide correct data interpretations. Readers are referred to Espitalié et al. 1985a, b, and c; Bordenave et al., (1993), Peters and Cassa, 1994, Lafargue et al. (1998), Behar et al. (2001) and McCarthy et al. (2011) for further details. Collectively, these scientific publications provide an in-depth guide on the application and interpretation of Rock-Eval data for use in petroleum exploration.

RE analysis was used in this study to assess changes in thermal maturity and geochemical properties of the source rocks before and after pyrolysis. The key RE parameters measured are S1 peak (free volatile hydrocarbons in mg HC/g rock), S2 peak (residual petroleum generation potential in mg HC/g rock), S3 peak (CO2 from organic source, in mg/g rock), TOC (total organic carbon in %), PC [total pyrolyzable carbon (S1+S2+S3)], HI [hydrogen index calculated as (S2 * 100/TOC) in mg HC/g TOC], OI [oxygen index calculated as (S3 * 100/TOC) in mg S3/g TOC], T_{max} (maximum temperature of the S2 peak, in ^{o}C) and PI [production index (S1/S1 + S2)]. These measured and calculated RE parameters are the most extensively used geochemical data in petroleum exploration (Espitalié et al. 1985a, b, and c; Lewan, 1985; Bordenave et al., 1993; Peters and Cassa, 1994; Lafargue et al., 1998; Behar et al., 2001; Peters et al., 2005a; McCarthy et al., 2011; Spigolon et al., 2015).

Hydrous Pyrolysis

Conventional closed hydrous pyrolysis uses large 500 to 1000 mL stainless steel Parr reactors with pressurized head space placed inside large electric heaters (Lewan, 1985). In this study, small stainless steel Swagelok plugs and caps (Figure 2) were used to build mini reactors (Hackley et al, 2013). The mini reactor has a total volume of 35 milliliters. For each pyrolysis, two-gram aliquots of the homogenized crushed rocks (ca 2mm particle size) were placed inside the reactors. Five milliliters of distilled water was added in each reactor, enough to submerge the rock chips and keep the produced hydrocarbon separated from the rock. The pyrolysis was carried out inside a GC oven at isothermal temperatures of 310, 320, 330, 340 and 350 ^{o}C for 72 hours (Hackley et al., 2013). These temperatures are well within simulated thermogenic hydrocarbon generation window based on previous hydrous pyrolysis studies (Lewan, 1985; Lewan, 1993; Lewan and Ruble, 2002; Hackley et al, 2013; Spigolon et al., 2015). The advantages of this modified technique are that it can be done quickly and with a small amount of sample. The key disadvantage of this technique is its inability to capture, quantify and analyze the produced gas after the completion of hydrous pyrolysis.

Organic Solvent Extraction

Organic solvent extraction is also one of the most widely used procedures in organic geochemistry (Peters, 1986; Peters et al., 2005a; Peters et al., 2005b; Spigolon et al., 2015 and references therein). This process separates and concentrates most of the free hydrocarbons and soluble bitumen (asphaltite and ozocerite) stored in the rock matrix, leaving behind the residual hydrogen-rich reactive insoluble kerogen and non-reactive organic carbon (Peters et al., 2005a; Peters et al., 2005b and references therein). In this study, organic solvent extraction was performed using Soxhlet apparatus with dichloromethane (DCM) as solvent and heated at 40 ^{o}C for 24 hours.

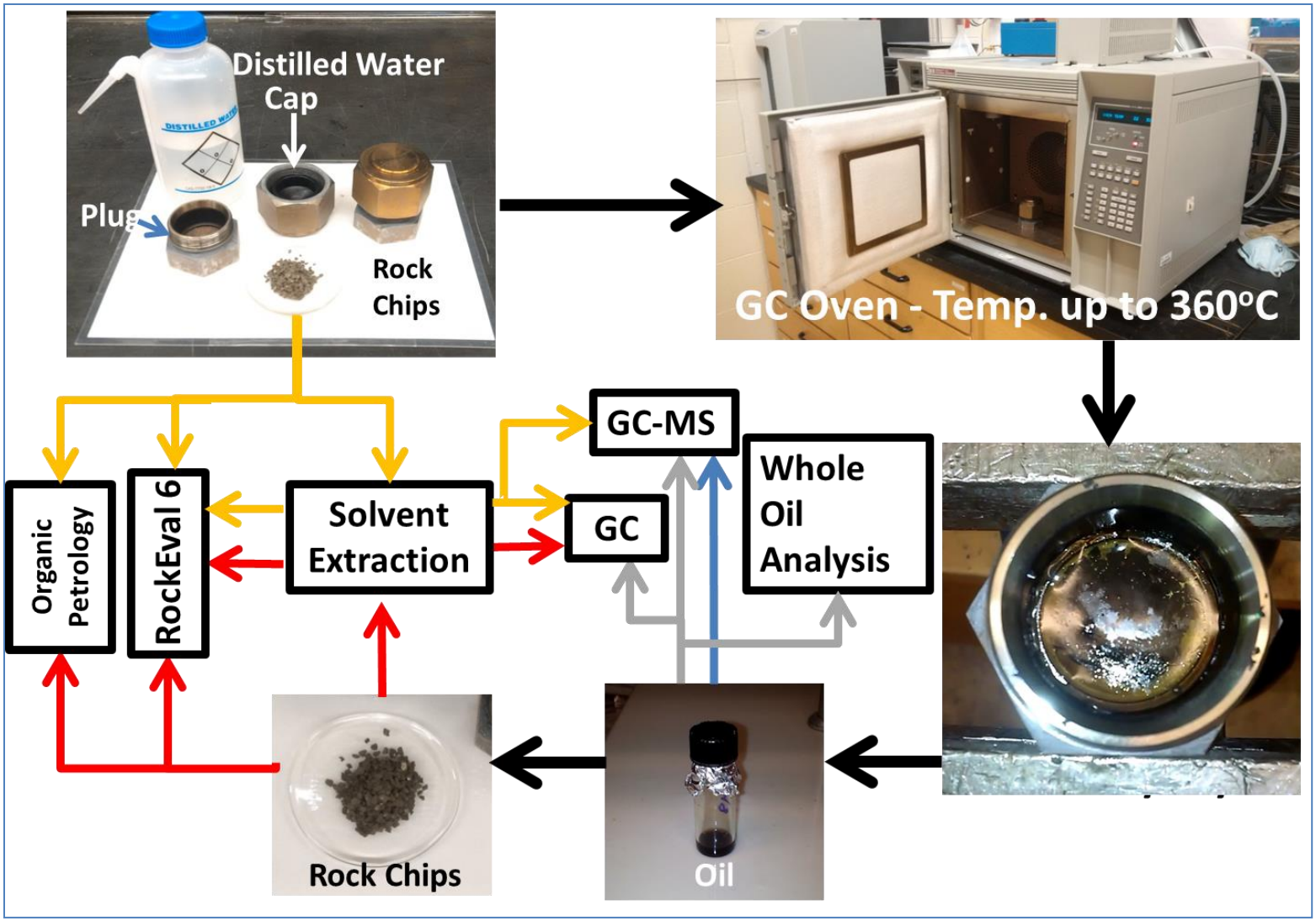

Figure 2. Simplified diagram showing modified hydrous pyrolysis technique and subsequent geochemical and organic petrographic analyses performed on the various aliquots before and after each stage of hydrous pyrolysis.

RESULTS AND DISCUSSION

Original Samples

RockEval Results

The TOC contents of the organic-rich shale samples of Amadjuak, Akpatok, Boas River and Red Head Rapids formations are 11.04, 3.14, 7.69 and 10.36 %, respectively (Table 1), with corresponding pyrolyzable carbon values of 5.85, 1.74, 4.17 and 5.60 (%). S1 is measured at 2.42, 0.86, 2.00 and 2.14 (mg/g rock) for Amadjuak, Akpatok, Boas River and Red Head Rapids formations, respectively (Table 1), and corresponding S2 values are 66.56, 19.64, 47.36 and 63.97 (mg/g rock), respectively. The hydrogen index (HI) ranges from 603 to 625 mg HC/ g TOC and the oxygen index (OI) ranges from 13 to 19 mg HC/g TOC (Table 1). Their measured T_{max} values are 421, 423, 424 and 413 ^{o}C (Table 1). The PI ranges from 0.03 to 0.04 (S1/ S1+S2) and calculated S2:S3 ratios range between 32 and 46 (Table 1).

The pseudo Van Krevelen diagram shows that these samples are Type II-1 kerogen (Figure 3) most likely deposited in an anoxic marine environment. All the key sources rock evaluation parameters (TOC, S2, and S1) indicate that these Upper Ordovician samples have very good to excellent hydrocarbon generation potential. The measured and calculated thermal maturity and oil generation parameters (Tmax, PI, S2:S3, Table 1) show that they are indeed immature to marginally mature source rocks according to widely recognized source rock evaluation criteria by Peters and Cassa (1994) and McCarthy et al. (2011).

Organic Petrography

Qualitative and semi-quantitative petrographic analysis shows that the most abundant organic macerals in these source rocks are amorphous kerogen and fluorescing and non-fluorescing bituminite derived from disseminated alginite (Figure 4). These are followed by

bright to weak yellow fluorescing alginite and prasinophyte-derived liptodetrinite disseminated throughout the rock matrices (Figure 4a-j), which can also be observed as inclusions within bituminite and amorphous kerogen laminae (Figure 4a-c). Similarly, disseminated non-fluorescing and bright to weak yellow fluorescing prasinophyte alginite [e.g. *Tasmanites sp*., *Leiosphaeridia sp*. and *Gloeocapsomorpha prisca* (G. prisca)] and acritarch (Figure 4b-f) were also observed in these formations. Significant to minor amounts of zooclast macerals including chitinozoan, graptolite, other calcareous macro-and micro-fossils (possibly conodont) were also identified in these units (Figure 4i-l).

It is important to recognize that the kerogen composition (organic facies) varies greatly among these formations. In general, the variations in kerogen composition are attributed to the dissimilarities in spatial, temporal and paleodepositional environment (Tyson, 1995; Stasiuk 1996; Stasiuk and Fowler, 2004; Peters et al., 2005a). The Boas River Formation mudstone has one of the highest concentrations of acritarch and chitinozoan zooclast in comparison to the other formations (Figure 4d, h-j). Trace amounts of graptolite and conodont microfossils were also identified in the Boas River Formation. The Akpatok Formation on the other hand has the highest concentration of large colonies of thick walled G. prisca and graptolites (Figure 4e-f, k-l) with trace amounts of chitinozoans. Both the Red Head Rapids and Amadjuak formations are dominated by amorphous kerogen and bituminite with rare amount of chitinozoans and calcareous microfossils (Figure 4k).

All these samples have rare to trace amounts of identifiable solid bitumen that can be accurately measured, except for the rare micro-size inclusions found in the bituminite matrix. Spheroidal matrix resembling bitumen and corpohuminite (Figure 4i) are possibly fragments of chitinozoan or species of small chitinozoan such as those presented in Jenkins (1970). In the graptolite-rich Akpatok Formation, some of the small spheroidal matrix appears to be small pieces of graptolite similar to one observed in Figure 4g.

Post Hydrous Pyrolysis

Table 1. Rock-Eval results of unextracted original and pyrolyzed rock samples including the calculated transformation ratio (TR) based on HI and S2 respectively, and the amount of hydrocarbon expelled and collected in the water column.

Sample Name & Location	Prolysis Temperature	Qty	TOC	Tmax	S1	S2	S3	PI	S2/S3	PC	HI	OI	TR HI	TR S2	$^{\#}HC_{expelled}$
	(°C)	(mg)	(%)	(°C)	(mg/g rock)	(mg/g rock)	(mg/g rock)	(S1/S1+S2)	S2/S3	(%)	(mg S2/g TOC	(mg S3/g TOC)	%	%	(mg HC/g TOC)
11SZ-10-18BB = Amadjuak Formation	Original	70.7	11.04	421	2.42	66.56	2.08	0.04	32.00	5.85	603	19	0	0	0
	310	70.3	9.65	432	6.29	49.08	0.20	0.11	245.40	4.67	509	2	16	26	nw*
	320	70.6	9.10	435	7.48	40.85	0.17	0.15	240.29	4.04	449	2	26	39	37.64
	330	70.4	8.65	438	7.44	30.43	0.25	0.20	121.72	3.17	352	3	42	54	63.41
	340	70.1	7.89	442	7.03	19.93	0.43	0.26	46.35	2.28	253	5	58	70	95.53
	350	70.6	7.37	448	7.02	14.75	0.21	0.32	70.24	1.85	200	3	67	78	152.85
SZ14-03A-01R = Akpatok Formation	Original	70.7	3.14	423	0.86	19.64	0.60	0.04	32.73	1.74	625	19	0	0	0.00
	310	70.5	2.44	432	1.54	13.64	0.19	0.10	71.79	1.28	559	8	11	31	19.47
	320	70.8	2.13	435	1.79	9.03	0.30	0.17	30.10	0.94	424	14	32	54	nw
	330	70.5	1.86	439	1.20	6.31	0.29	0.16	21.76	0.65	339	16	46	68	102.28
	340	70.2	1.69	445	1.01	4.17	0.31	0.19	13.45	0.45	247	18	60	79	163.02
	350	70.3	1.61	450	1.02	2.96	0.25	0.26	11.84	0.35	184	16	71	85	139.13
11DKA024A06 = Boas River Formation	Original	70.3	7.69	424	2.00	47.36	1.03	0.04	45.98	4.17	616	13	0	0	0.00
	310	70.4	6.19	437	2.58	22.84	0.10	0.10	228.40	2.16	369	2	40	52	nw
	320	70.2	6.30	438	5.71	25.75	0.32	0.18	80.47	2.67	409	5	34	46	nw
	330	70.9	5.79	441	4.15	20.58	0.30	0.17	68.60	2.09	355	5	42	57	22.75
	340	70.2	5.52	445	4.41	15.71	0.26	0.22	60.42	1.70	285	5	54	67	56.93
	350	70.5	5.54	450	5.97	12.06	0.21	0.33	57.43	1.52	218	4	65	75	51.74
SZ14-26-01 = Red Head Rapids Formation	Original	70.2	10.36	413	2.14	63.97	1.71	0.03	37.41	5.60	617	17	0	0	0.00
	310	70.6	8.70	431	6.65	41.85	0.18	0.14	232.50	4.06	481	2	22	35	nw
	320	70.1	8.11	435	8.14	32.17	0.30	0.20	107.23	3.39	397	4	36	50	68.59
	330	50.7	7.16	440	6.46	20.97	0.30	0.24	69.90	2.32	293	4	53	67	77.69
	340	70.3	6.72	445	5.91	14.84	0.30	0.28	49.47	1.77	221	4	64	77	166.22
	350	70.3	6.81	449	6.87	11.35	0.22	0.38	51.59	1.55	167	3	73	82	108.92

***nw = no weight recorded; $^{\#}$collected from the ware column after hydrous pyrolysis; *S1 = free volatile hydrocarbons (in mg HC/g rock); S2 = residual petroleum generation potential (in mg HC/g rock); TOC = total organic carbon (%); PC = total pyrolyzable carbon (S1+S2+S3); HI = hydrogen index (S2 * 100/TOC; in mg HC/g TOC); OI = oxygen index (S3 * 100/TOC; in mg S3/g TOC); S3 = CO2 from organic source (in mg/g rock); Tmax = maximum temperature at S2 peak (in oC); PI = production index (S1/S1 + S2) ; TRS2 = (S2original – S2residual)/(S2original)*100; TRHI = (HIoriginal – HIresidual) / HIoriginal)*100**

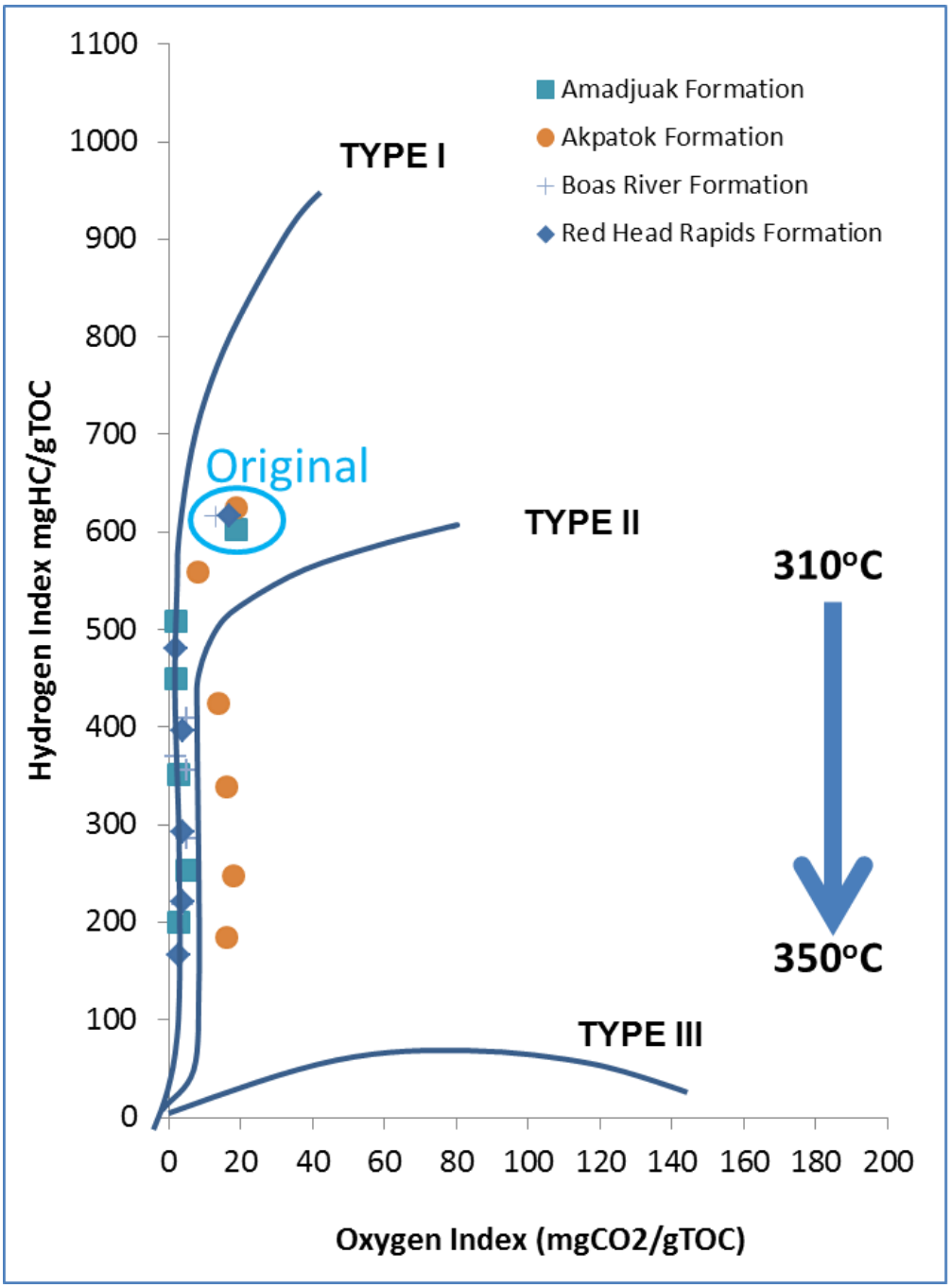

Figure 3. Pseudo Van Krevelen Diagram showing Kerogen Type before and after hydrous pyrolysis. Values circled in blue are the original in-situ outcrop samples.

Rock-Eval Results

The key RE parameter used to determine the thermal maturity of source rocks in relation to its hydrocarbon generation potential is the T_{max} (Peters and Cassa, 1994; Lafargue et al., 1998; Behar et al., 2001; Peters et al., 2005a, McCarthy et al., 2011). The measured T_{max} increased to 431-437 ^{o}C and 448-450 ^{o}C from the original 413 to 424 ^{o}C values, after pyrolysis at 310 ^{o}C and 350 ^{o}C for 72 hours, respectively. The Boas River Formation sample reached maturity for hydrocarbon generation (T_{max} = 435-465 ^{o}C, Peters and Cassa, 1994 and McCarthy et al., 2011) with a measured T_{max} of 437 ^{o}C after the first pyrolysis step (310 ^{o}C). The Amadjuak, Akpatok and Red Head Rapids formations samples reached early maturity (431-432 ^{o}C) after the 310 ^{o}C pyrolysis. The removal of solvent-extractable soluble organics and subsequent Rock-Eval analysis indicates that all samples reached hydrocarbon generation with T_{max} ≥435 ^{o}C after 310 ^{o}C pyrolysis (Figure 5 and Table 2). These T_{max} values are much higher than the values for unextracted samples presented in Table 1 and Figure 6. Once again, Boas River Formation samples have a higher T_{max} (441 ^{o}C) than the samples from the other formations (435-436 ^{o}C). The pyrograms in Figure 5 clearly show that the T_{max} increased after the removal of soluble organics. Tables 1 and 2, as well as Figure 6, show that the Tmax of extracted samples are consistently higher compared to the unextracted samples at every pyrolysis temperature point.

Using the equation of Jarvie et al (2001) [T_{maxeq}, %Ro = 0.018(T_{max}) – 7.16], the calculated VR_{eqv} of the measured T_{max} of the extracted samples (Table 2) is between 0.67 to 1.03 $\%Ro_{eqv}$. The estimated peak burial heating temperatures required to reach these values of Tmax and VR_{eqv} are 104 to 131 ^{o}C according to Barker and Pawlewicz (1994). All formations show strong positive linear correlations ($R^2 \geq 0.86$) between Tmax values and pyrolysis temperatures for both unextracted and extracted pyrolyzates (Figure 6), indicating that all samples have been artificially matured.

It is important to note that in Rock-Eval 6, the standard relative peak temperature, Tmax, (Figure 5) is calculated using the equation TpS2 – ΔT_{max} after the S2 peak maximum (Tpeak) is reached, (Behar et al., 2001). This correction is necessary to compensate for the difference in apparatus setup between the Rock-Eval 2 and Rock-Eval 6 (Espitalié et al., 1985a, b, c). In the Rock-Eval 2, the temperature probe measures the oven temperature

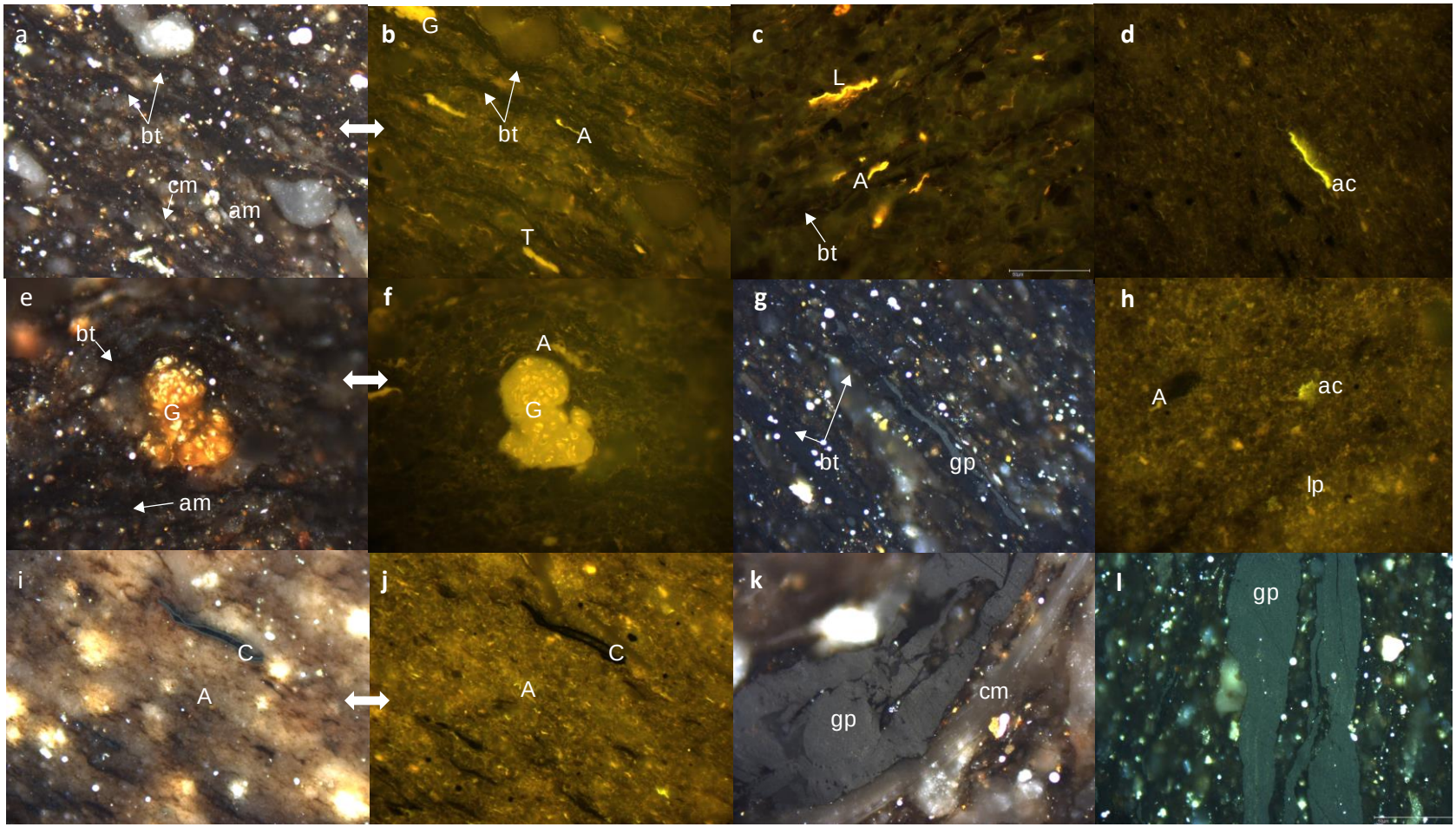

Figure 4. Photomicrographs showing variations in dispersed organic matter (DOM), arrows indicate the same image under white and UV light. a-c) Amorphous kerogen (am) and weak fluorescing bituminite (bt) with yellow fluorescing alginite [A, *Tasmanites sp.* (T), *Leiosphaeridia sp.* (L)] inclusions. d) Dispersed fine grained, weak fluorescing liptodetrinite (lp) with bright greenish yellow fluorescing acritarch (ac) inclusion. e-f) Large colony of G. Prisca (G) surrounded by granular bituminite (bt), amorphous (am) kerogen and disseminated fluorescing alginite (A). g-h) Organic rich matrix showing bituminite and graptolite (gp) zooclast and acritarch (ac) with weak yellow fluorescing disseminated liptodetrinite (lp) and bright yellow fluorescing alginite (A). i-j) Chitinozoan with small prasinophyte alginite (A) in mudstone matrix. k-l) Large graptolite (gp) and calcareous microfossils (cm, conodonts?) in organic rich matrix. Reflected white and UV light in oil, 50 x magnifications, scale 50 microns.

whereas in the Rock-Eval 6 the probe measures the effective temperature of the sample. Rock-Eval 6 provides a more accurate measurement of the effective T_{max} (Behar et al., 2001).

The differences in measured T_{max} amongst these formations may be attributed to the variations in thermal conductivity due to varying lithology and mineralogy (Espitalié et al., 1980; Yang and Horsfield 2016). Shale has much lower thermal conductivity than limestone (Clark, 1966; Blackwell and Steele, 1989; Eppelbaum et al., 2014). These differences in thermal conductivity may delay thermal maturation of organic rich shales compared to organic lean limestones under the same thermal regime (McTavish, 1998). The overall kerogen type found the source rocks can also affect the T_{max} (McCarthy et al., 2011) due to the variation in activation energy of the different kerogen macerals (Petersen et al., 2004; Hakimi et al., 2015). In general, lacustrine deposits have lower and narrow activation energy distributions than marine deposits (Tissot et al., 1987, Jarvie, 1991; Pepper and Corvit, 1994; Tegelaar and Noble, 1994; Petersen et al., 2002; Petersen et al., 2004)

S2 and TOC (Table 1, Figure 7 and Figure 8) decrease with increasing pyrolysis temperature, in contrast to S1 (Table 1, Figure 9). S2 values decline from 19.64-66.56 mg HC/g rock (original) to 2.96-14.75 mg HC/g rock after the last stage of hydrous pyrolysis (Table 1). The best-fitting regression lines indicate a strong negative (exponential) correlation (R^2 = 0.84 to 1.00) between S2 and pyrolysis temperature (Figure 7). S2 decreases for all formations after extraction (Table 2 and Figure 7). The RE pyrograms (Figure 5) clearly illustrate the significant decrease in the main S2 peak area and the disappearance of the small front shoulder in comparison to the unextracted pyrolyzed rock chips. This suggests that large quantities of residual labile hydrocarbon and soluble bitumen are present in the $S2_{unextracted}$ peak. Figure 7 also illustrates the exponential rate of thermal decomposition of H-rich insoluble kerogen to petroleum products such as soluble bitumen, free hydrocarbons, gas and pyrobitumen.

The TOC content of samples from the Amadjuak, Akpatok, Boas River and Red Head Rapids formations decreased from 11.04 to 7.37, 3.14 to 1.61, 7.69 to 5.54 and 10.36 to 6.81 (%), respectively, after the last stage of pyrolysis at 350 °C (Table 1). As expected, the subsequent removal of extractable soluble organics further decreased the TOC (Table 2, Figure 8). This is clearly illustrated in Figure 5b by the significant decline in S1 and S2

Table 2. Rock-Eval results of extracted un-pyrolyzed original and pyrolyzed source rock samples including the calculated transformation ratio (TR) of the measured S2 and calculated HI.

Sample Name & Location	Prolysis Temperature	Qty	TOC	Tmax	S1	S2	S3	PI	S2/S3	PC	HI	OI	TR HI	TR S2
	(°C)	(mg)	(%)	(°C)	(mg/g rock)	(mg/g rock)	(mg/g rock)	(S1/S1+S2)	S2/S3	(%)	(mg S2/g TOC	(mg S3/g TOC)	%	%
11SZ-10-18BB = Amadjuak Formation	Original	70.7	10.27	421	0.41	60.34	2.11	0.01	28.60	5.18	588	21	na	na
	310	70.3	7.43	436	0.13	31.97	0.15	0.00	213.13	2.70	430	2	27	47
	320	70.3	6.80	439	0.16	21.87	0.16	0.01	136.69	1.86	322	2	45	64
	330	50.8	5.13	439	0.09	14.48	0.24	0.01	60.33	1.26	282	5	52	76
	340	40.5	6.39	446	0.22	10.88	0.34	0.02	32.00	0.97	170	5	71	82
	350	50.4	5.94	451	0.15	7.34	0.31	0.02	23.68	0.66	124	5	79	88
SZ14-03A-01R = Akpatok Formation	Original	70.8	2.85	424	0.09	18.51	0.73	0.00	25.36	1.60	605	26	na	na
	310	71.0	1.70	436	0.03	8.04	0.21	0.00	38.29	0.69	473	12	22	57
	320	69.8	1.47	439	0.04	5.38	0.22	0.01	24.45	0.47	366	15	40	71
	330	70.8	1.34	443	0.04	3.76	0.21	0.01	17.90	0.33	281	16	54	80
	340	70.5	1.37	446	0.02	2.33	0.28	0.01	8.32	0.22	170	20	72	87
	350	70.7	1.32	452	0.02	1.57	0.21	0.01	7.48	0.15	119	16	80	92
11DKA024A06 = Boas River Formation	Original	70.1	7.61	425	0.26	44.44	1.27	0.01	34.99	3.82	584	17	na	na
	310	50.4	4.57	441	0.26	15.76	0.27	0.02	58.37	1.37	240	4	59	65
	320	50.3	4.43	440	0.19	14.17	0.26	0.01	54.50	1.23	320	6	45	68
	330	50.9	4.26	444	0.15	11.63	0.25	0.01	46.52	1.02	273	6	53	74
	340	71.0	4.46	447	0.18	9.51	0.22	0.02	43.23	0.84	213	5	64	79
	350	70.2	4.28	454	0.14	6.31	0.22	0.02	28.68	0.56	147	5	75	86
SZ14-26-01 = Red Head Rapids Formation	Original	70.5	9.63	415	0.50	57.21	1.88	0.01	30.43	4.93	594	20	na	na
	310	71.0	6.32	435	0.22	22.77	0.22	0.01	103.50	1.94	360	3	39	60
	320	70.6	5.82	439	0.43	16.91	0.30	0.02	56.37	1.48	291	5	51	70
	330	70.4	5.50	443	0.28	11.32	0.30	0.02	37.73	1.01	206	5	65	80
	340	69.9	5.41	448	0.22	8.44	0.27	0.03	31.26	0.76	156	5	74	85
	350	71.0	5.62	455	0.17	5.97	0.19	0.03	31.42	0.54	106	3	82	90

NA = Not avialable

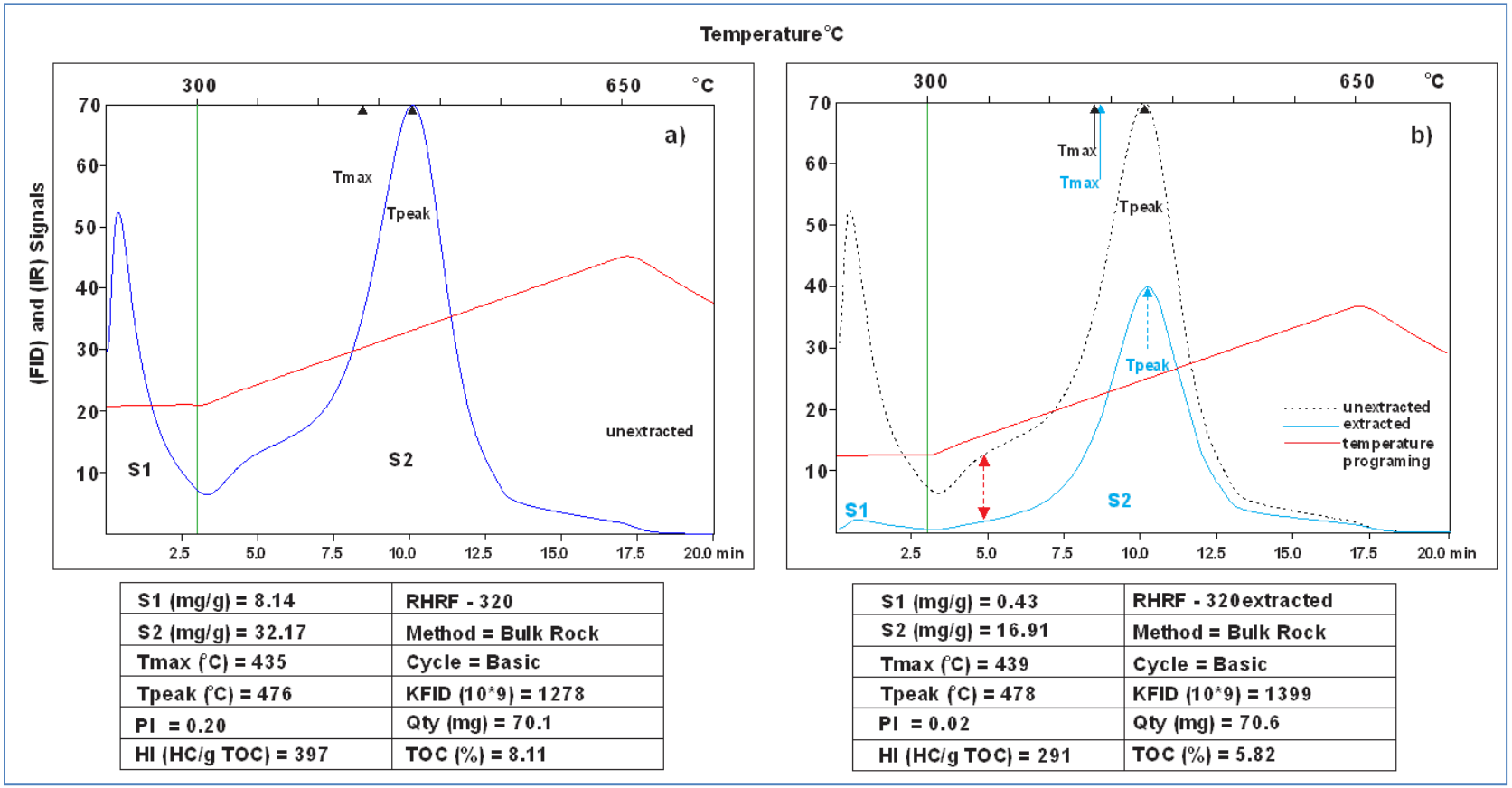

S1 (mg/g) = 8.14	RHRF - 320
S2 (mg/g) = 32.17	Method = Bulk Rock
Tmax (°C) = 435	Cycle = Basic
Tpeak (°C) = 476	KFID (10*9) = 1278
PI = 0.20	Qty (mg) = 70.1
HI (HC/g TOC) = 397	TOC (%) = 8.11

S1 (mg/g) = 0.43	RHRF - 320extracted
S2 (mg/g) = 16.91	Method = Bulk Rock
Tmax (°C) = 439	Cycle = Basic
Tpeak (°C) = 478	KFID (10*9) = 1399
PI = 0.02	Qty (mg) = 70.6
HI (HC/g TOC) = 291	TOC (%) = 5.82

Figure 5. Typical Rock-Eval pyrograms (Read Head Rapids Formation) after hydrous pyrolysis at 320 °C, before (a) and after (b) organic solvent extraction. The extraction removes extractable organic matter such as free hydrocarbons and soluble organics (bitumen/asphaltite). The accompanying tables show some of the key RE parameters. a) Shows high amount S1 and S2 in the pyrolyzed source rocks. b) Pyrograms of extracted samples (solid blue curve) and unextracted pyrolyzed source rocks (dashed curve).

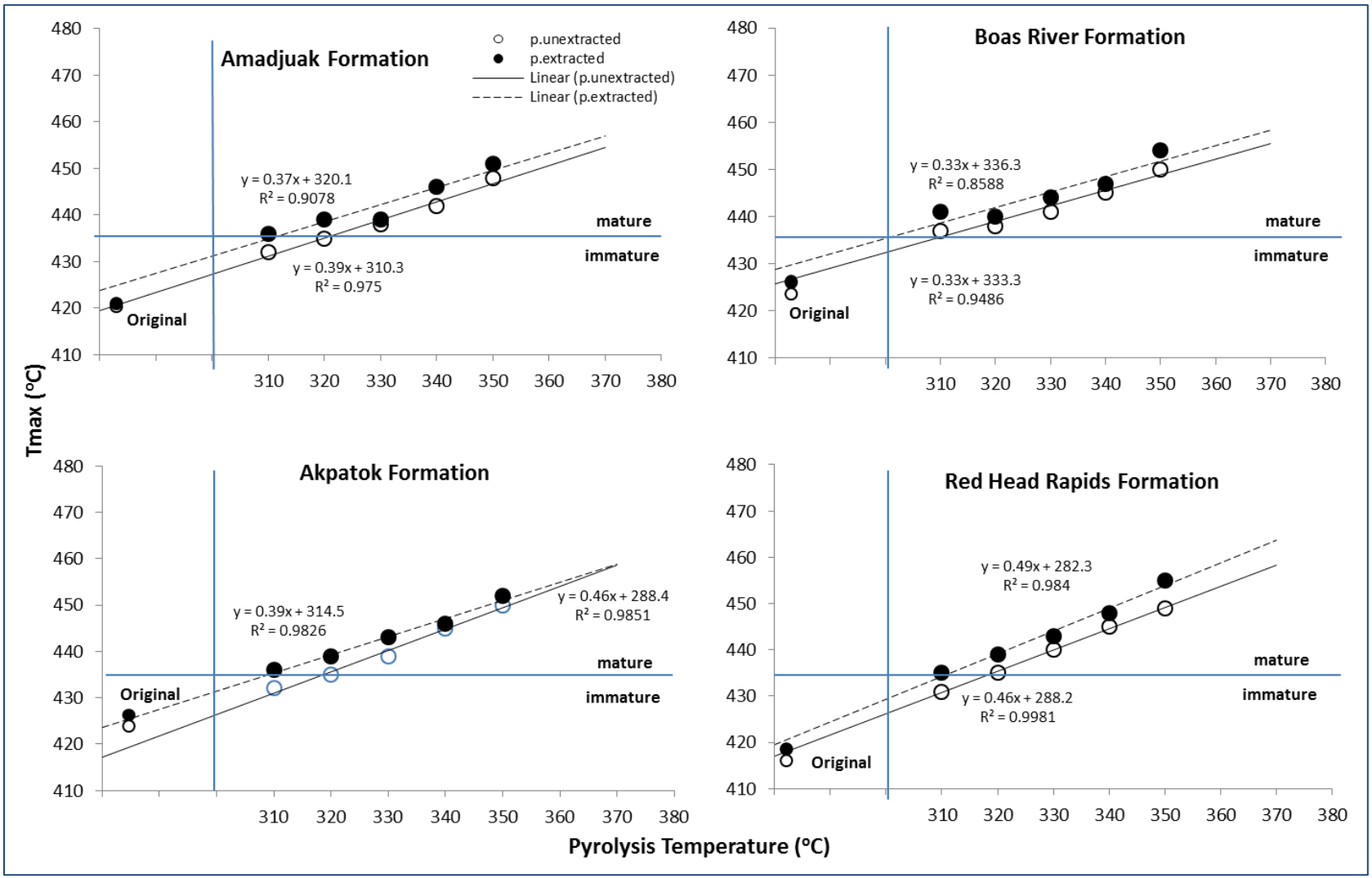

Figure 6. Rock-Eval T_{max} values of the original and pyrolyzed samples, before and after solvent extraction as a function of pyrolysis temperature. These graphs show increase in the thermal maturity after each stage of hydrous pyrolysis.

peaks, which represent the amount of free hydrocarbons and soluble bitumen extracted from the pyrolyzed rock chips. It is important to note that the TOC is the combined total of the free hydrocarbons (S1), soluble heavy organic and insoluble reactive kerogen (S2) and non-reactive residual carbon in the source rocks (Peters and Cassa; 1994; Lafargue et al., 1998; McCarthy et al., 2011). Although large quantities of hydrocarbons were expelled into the water phase, some of the free hydrocarbons remained and re-adsorbed in the rock matrix together with soluble bitumen (i.e. asphaltite). As the thermal maturity continues to increase, this soluble solid bitumen will continue to thermally crack into hydrocarbon, gas and insoluble pyrobitumen (Jacob, 1989; Jacob, 1993). The formation and accumulation of insoluble pyrobitumen contributes to the subsequent minor increase in TOC content of the extracted samples as the thermal maturity increase results in a polynomial rather than exponential trend (Figure 8). The removal of solvent-extractable soluble organics provides a more accurate representation of the correlation between residual TOC (reactive and non-reactive) and pyrolysis temperature (Figure 8) in comparison to the unextracted samples.

S1 (mg HC /mg rock) measures the amount of free hydrocarbons retained in the source rocks or in the reservoirs. It is one of the key parameters used to evaluate the hydrocarbon potential of source rocks (Lewan, 1985; Peters and Cassa, 1994; Lafargue et al., 1998; Behar et al., 2001; Peters et al., 2005b; McCarthy et al., 2011, Spigolon et al., 2015). The S1 values increase to 1.02 – 7.02 HC/ g rock at 350 ^{o}C from the original 0.86 - 2.42 mg HC/ g rock (Table 1). The increased in S1 values indicates that hydrocarbons have been generated during hydrous pyrolysis. Figure 9 illustrates that the hydrocarbon retention rate varies slightly between the formations, with the Akpatok Formation having the lowest. The difference in retention may be due to matrix porosity variance and unrecognized possible post pyrolysis sample processing error. Rock-Eval results of extracted samples indicate that a significant portion of S1 was removed by organic solvent extraction from all the formations (Table 2, Figure 9). Figure 5b clearly shows a significant decrease in S1 peak after extraction in comparison to the unextracted samples (Figure 5a). These changes are all attributed to the removal of S1 free hydrocarbons from the rock matrix.

The subsequent decline in S1 after reaching peak hydrocarbon generation corresponds to the increase in hydrocarbon expulsion as noted in Table 1, as well as the thermal cracking

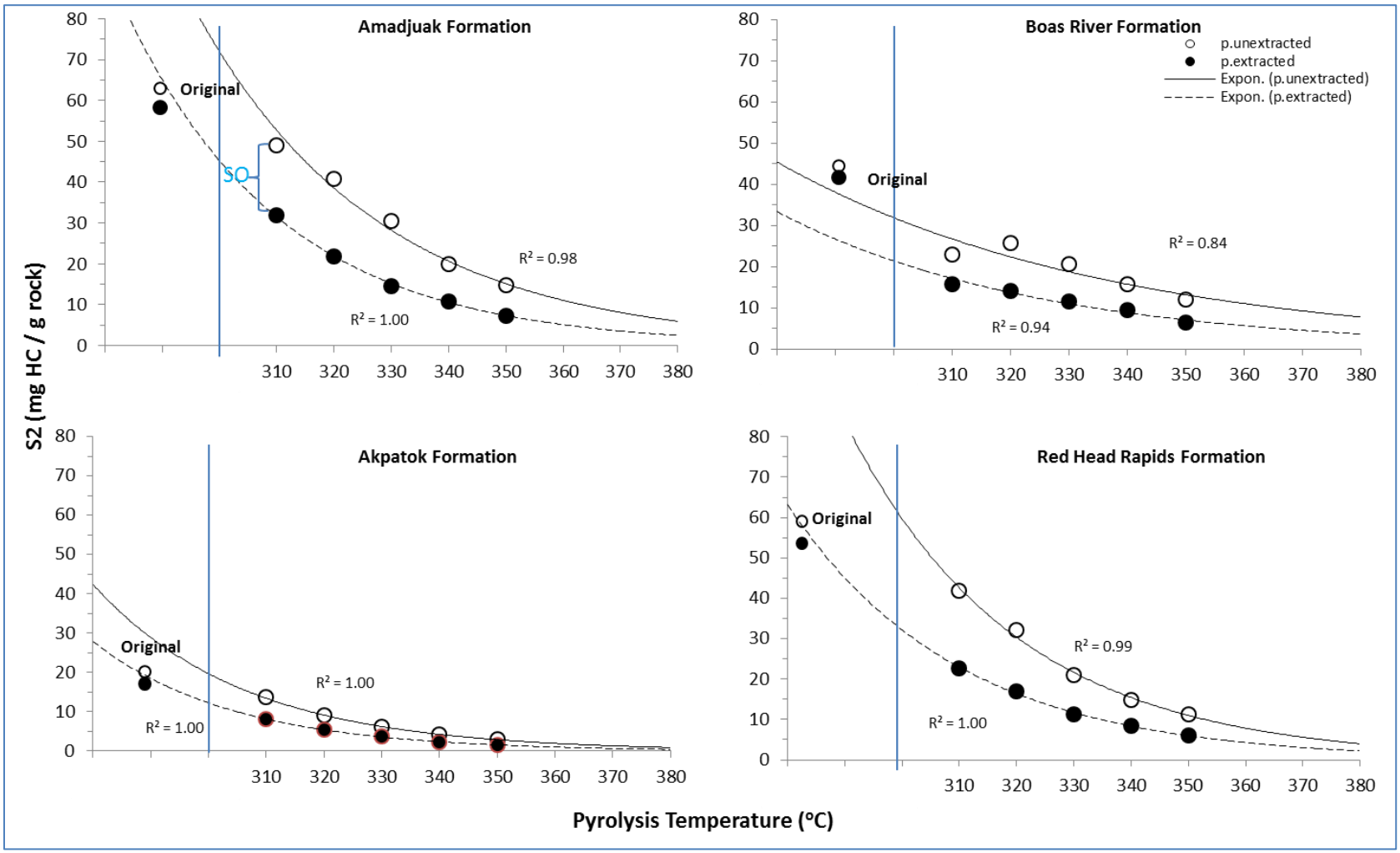

Figure 7. Variation of Rock-Eval S2 values with pyrolysis temperature for both non-extracted and extracted pyrolyzed samples in this study. SO are soluble organics (bitumen, i.e. asphaltite) and labile hydrocarbons present in tight pore spaces in the S2 that cannot be released into S1 peak but can be solvent-extracted.

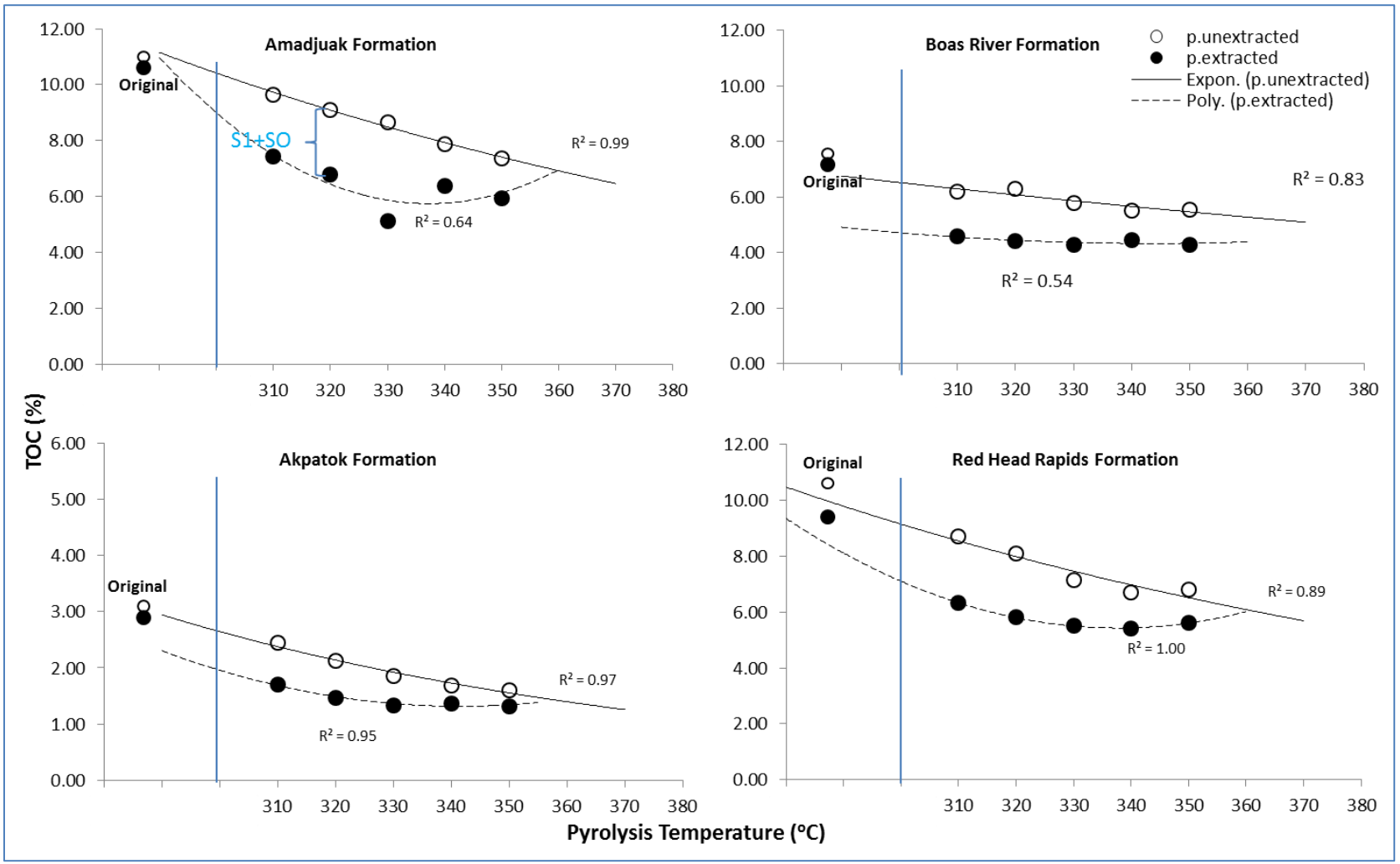

Figure 8. Variation of TOC content with pyrolysis temperature for both non-extracted and extracted pyrolyzed samples. S1+SO are the amount of labile hydrocarbon and soluble organic in S2 matter in the solid residues from pyrolysis.

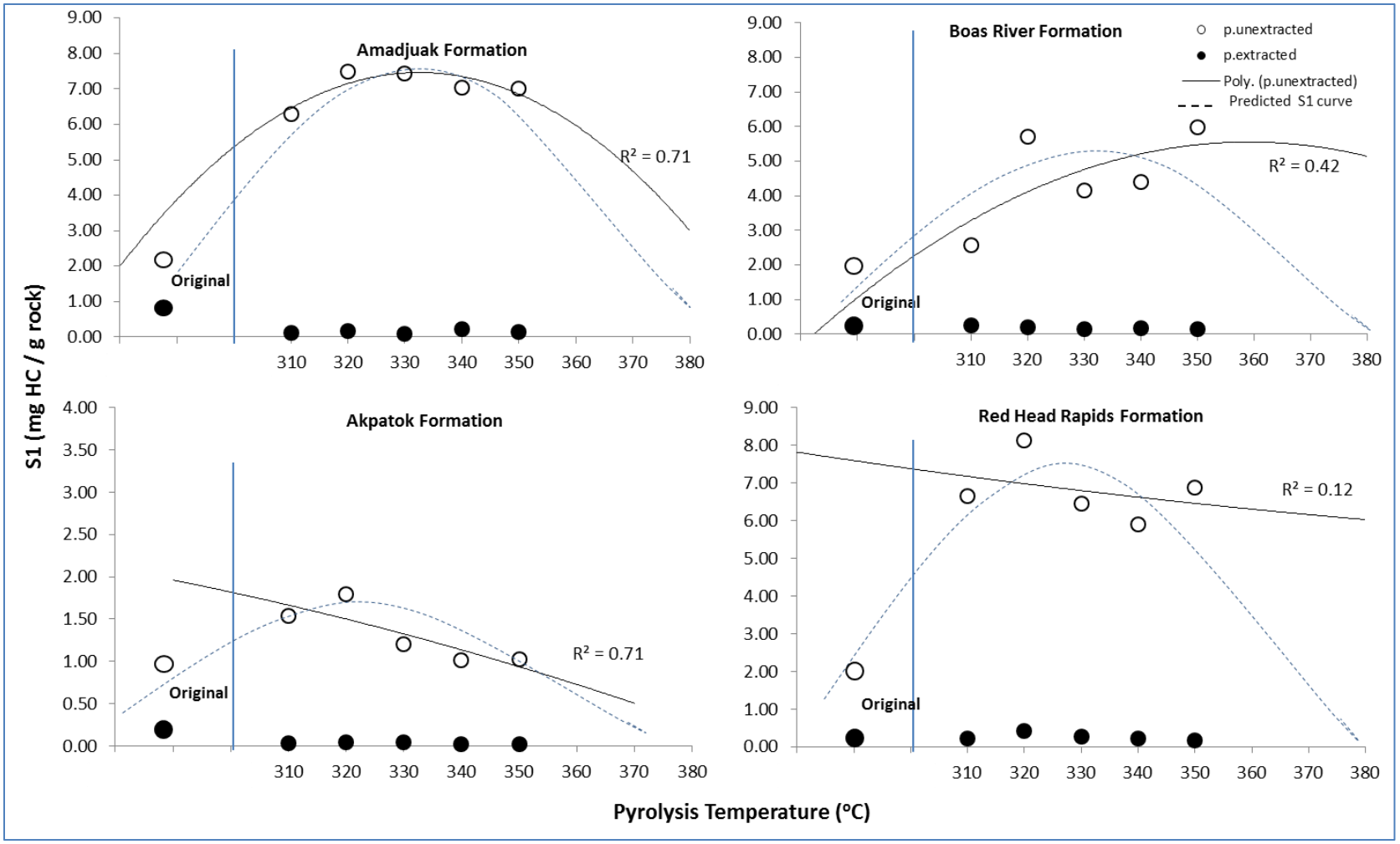

Figure 9. Rock-Eval S1 after hydrous pyrolysis, before and after solvent extraction as a function of pyrolysis temperature (°C). These graphs show the concentration of free hydrocarbons adsorbed and stored in rock matrix after each stage of hydrous pyrolysis. Predicted S1 curve is based on the original S1values and its subsequent decline with increasing thermal maturity.

of liquid hydrocarbons to gaseous hydrocarbons. The predicted S1 curves (Figure 9) illustrate the production rate of S2-derived hydrocarbons from the start of hydrocarbon generation during the catagenesis and into the gas window. As expected, the increase in S1 (Figure 9) is inversely related to the decrease in S2 (Figure 7), since S1 is a by-product of the thermal degradation of kerogen (S2) (Tissot and Welte, 1984; Lafargue et al., 1998; Behar et al., 2001; McCarthy et al., 2011).

In the subsurface, the amount of in-situ S1 in the source rocks will depend upon the availability of migration pathways during and after hydrocarbon generation (Tissot and Welte, 1981; Noble et al., 1991; Peters, and Cassa, 1994). If the amount of S1 in the rock matrix exceeds that of the S2, possible hydrocarbon migration (Tissot and Welte, 1984) or contamination (Lafargue et al., 1998; Tissot and Welte, 1984) may have occurred.

Hydrogen index decreased from 603-625 mg HC/g TOC (original) to 167-218 mg HC/g TOC (Table 1, Figure 10) after 350 °C pyrolysis. All formations show a strong negative linear correlation between HI and pyrolysis temperature with the exception of the Boas River Formation (Figure 10) due to the significantly lower HI after the 310 ^{o}C pyrolysis step. Since all the samples have very similar HI values prior to hydrous pyrolysis, it would suggest that a higher percentage of the hydrogen was released by the sample from the Boas River Formation compared to the other formations after the 310 ^{o}C pyrolysis step in comparison to the other samples. The amount of hydrocarbons collected in liquid pyrolyzates (Table 1) and S1 (Figure 9) in the pyrolyzed residues suggest that some hydrogen was converted into gas. Unfortunately, due to the physical limitation of this modified hydrous pyrolysis, the amount of produced gas was not quantified. After the solvent extraction, the HI decreased significantly as the heavy free hydrocarbons and soluble bitumen were removed (Table 2 and Figure 10) from the rock matrix. The extraction of free hydrocarbons and soluble bitumen illustrate that the relationship between the HI and temperature is curvilinear (exponential $R^2 \geq 0.98$) rather than linear (Figure 10).

The calculated PI increased exponentially from 0.03-0.04 to 0.26-0.38 with increasing pyrolysis temperature (Table 1 and Figure 11). The increase in PI is the direct result of the conversion of the reactive insoluble kerogen (S2) into free hydrocarbons (S1) during

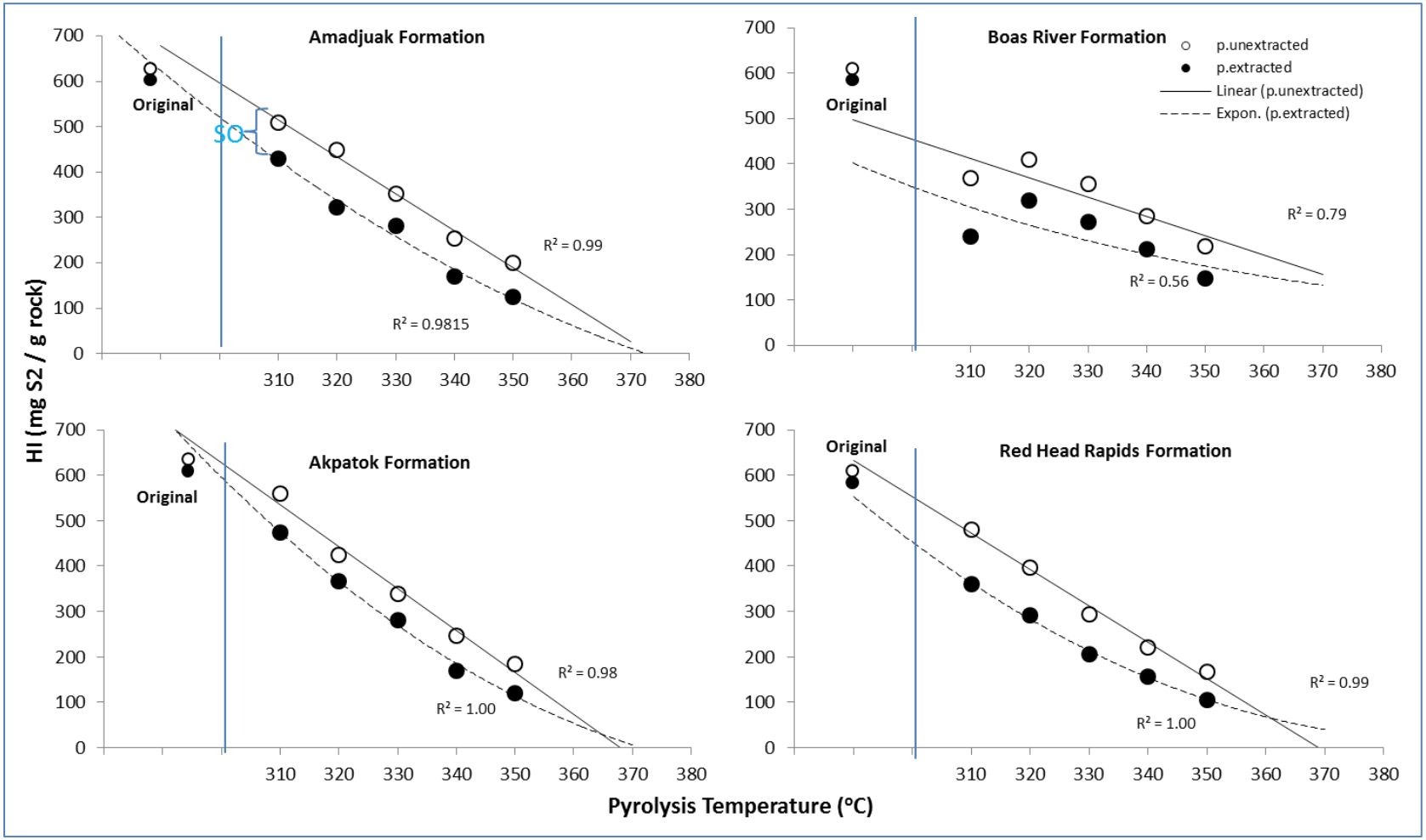

Figure 10. Calculated hydrogen index (HI) after hydrous pyrolysis, before and after solvent extraction as a function of pyrolysis temperature. SO represents the quantity of un-expelled free hydrocarbons and soluble organics (bitumen, i.e. asphaltite) removed by the solvent extraction.

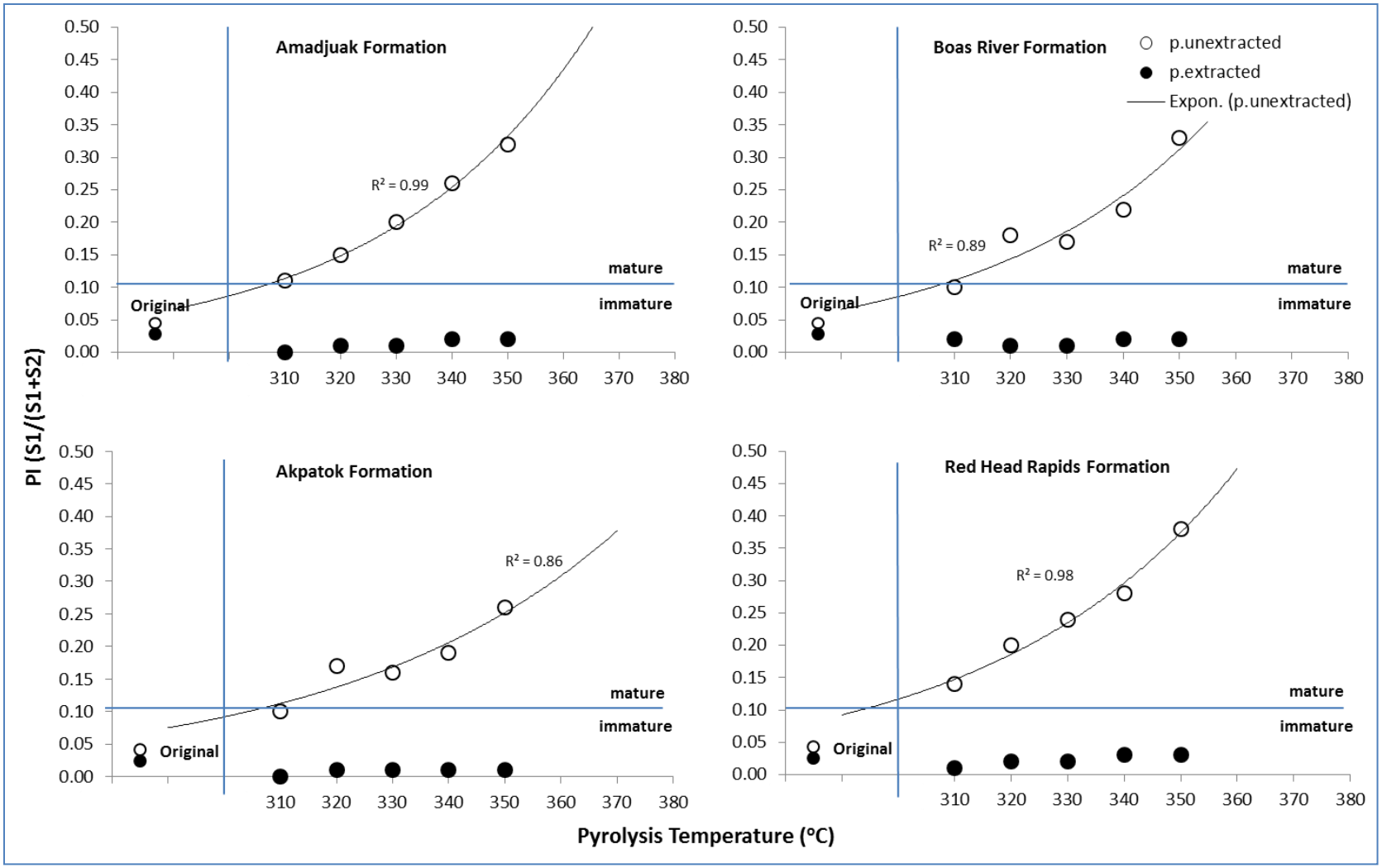

Figure 11. Calculated production index (PI) after pyrolysis, before and after solvent extraction as a function of pyrolysis temperature (^{o}C). These graphs show the concentration of free hydrocarbons adsorbed in the rock matrix after each stage of hydrous pyrolysis and solvent extraction.

thermal degradation of reactive kerogen (Lewan, 1985; Lafargue et al., 1998; Behar et al., 2001; McCarthy et al., 2011; Spigolon et al., 2015). The PI clearly indicates that all formations are immature (PI <0.10, Peters and Cassa, 1994; McCarthy et al., 2011) prior to hydrous pyrolysis. Only after the first pyrolysis step that all the formations reached HCG level of maturity (PI = 0.10-0.40, Peters and Cassa, 1994; McCarthy et al., 2011) (Figure 11).

Pyrolyzable carbon (PC) decreased from 1.74-5.85 to 0.35-1.85 % (Table 1) after hydrous pyrolysis, a similar decrease is observed for the solvent extracted pyrolyzed samples (Table 2). The overall decline in PC is also the direct result of the thermal degradation and transformation of kerogen. The percentage of PC decreases significantly with the extraction of S1 and S2-bound extractable organic matter (Figure 12).

The as received S2:S3 ratio (32.0- 46.0) also indicates that these samples are immature oil (S2:S3 >5, Peter and Cassa, 1994) prone Type II-IS kerogen. After the 310°C pyrolysis the S2:S3 ratio increased to 71.8-245.4 but gradually decreased to 11.8-70.2 after 350 ^{o}C (Table 1). The initial increased in S2:S3 ratio can be attributed to the sharp declined in S3 after the 310 ^{o}C pyrolysis in comparison to the S2 concentration (Table 1). The subsequent decreased in S2:S3 ratios were direct results of exponential degradation of S2 and increase expulsion rate of the produced hydrocarbon while the S3 remained the generally same.

The high S2:S3 ratios of the unextracted and extracted suggest that these samples are still immature after the last pyrolysis temperature of 350 °C. However, the combined analysis of the S2:S3 ratios, Tmax, PI and HI (Table 1) indicate that these samples did indeed thermally mature and have transformed into oil/gas prone kerogen from oil prone Type II-IS kerogen after 350 ^{o}C pyrolysis. The S2:S3 ratio will continue to decrease as the quantity of residual kerogen continues to decrease with increasing thermal maturity.

Organic petrology of pyrolyzed rock chips

Bituminite and amorphous kerogen (Figure 13a) were the first organic macerals to thermally decompose after the first stage of hydrous pyrolysis, which left behind large pore

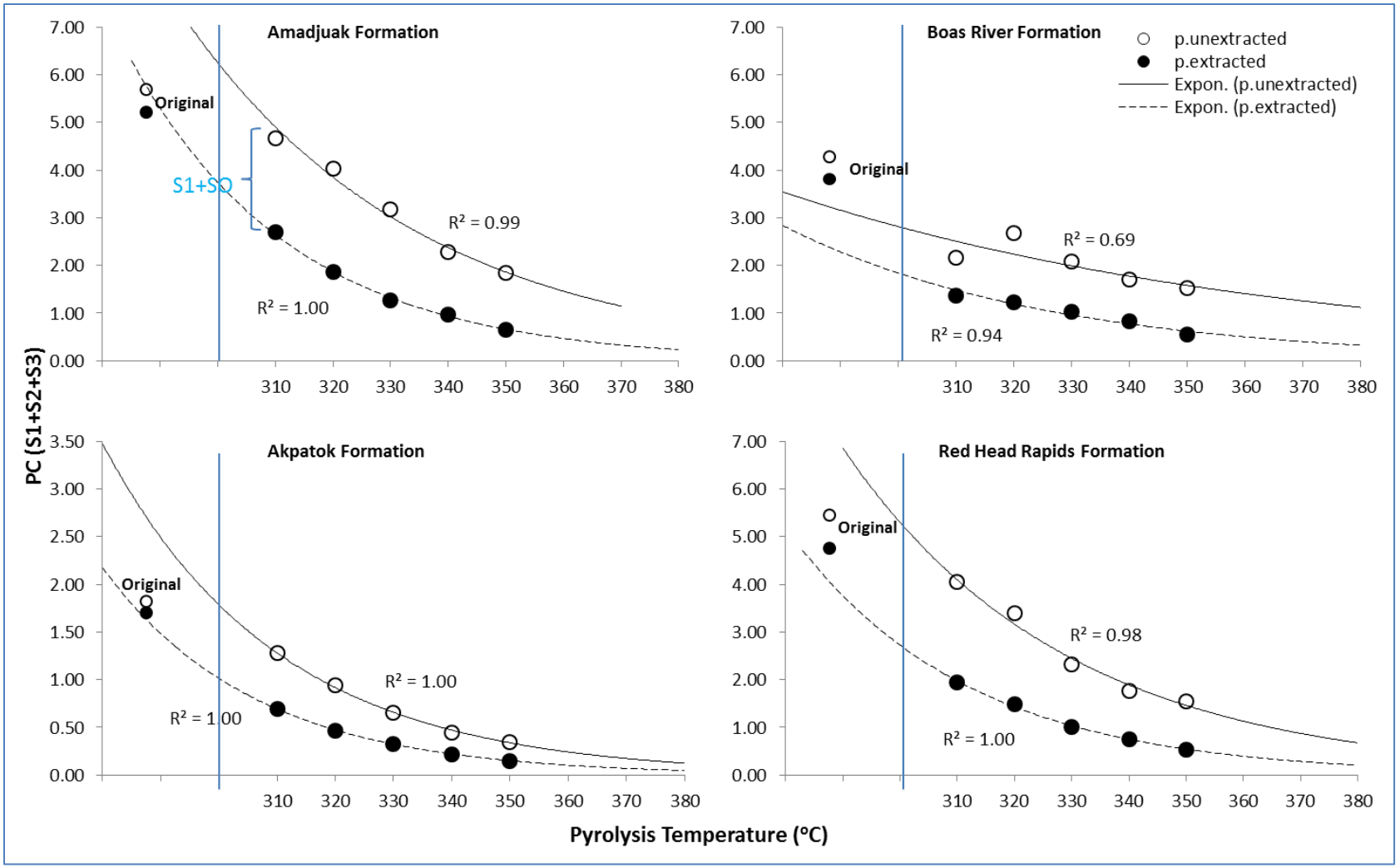

Figure 12. Calculated pyrolyzable carbon (PC) after hydrous pyrolysis, before and after solvent extraction as a function of pyrolysis temperature (^{o}C). S1 + SO represent the quantity of hydrocarbons and soluble organics (bitumen, i.e. asphaltite) stored in the rock samples.

spaces (Figure 13a-f). This was then followed by the decomposition of small, thin walled, weak fluorescing disseminated prasinophyte alginite (Figure 13b). The overall fluorescence properties of the alginite also change from bright yellow to weak orange fluorescence (Figure 13b). These changes in fluorescence properties are, at times, not easily discernable due to the high volume of bright fluorescing free hydrocarbons within the rock matrix (Figure 13b-d). The retained hydrocarbons were observed predominantly within fracture zones and intergranular pore spaces along the edges of the rock matrix (Figure 13b-c). Weakly orange fluorescing thick-walled *Tasmanites sp*. alginite can still be observed after 330 °C pyrolysis, some with bright fluorescing bitumen inclusions (Figure 13d). Some of the pore spaces vacated by the bituminite and amorphous kerogen were filled by fluorescing and non-fluorescing soluble bitumen (Figure 13c-e). Most of the observed bitumen rapidly dissolved and became mobile within seconds of being exposed to UV light under a confocal microscope, especially those formed at lower (310 to 330^{o}C) pyrolysis temperatures (Figure 13b-d). Together with the adsorbed free hydrocarbons they formed a thick bright fluorescing hydrocarbon layer on the surface of the rock matrix (Figure 13b-d). As the pyrolysis temperature increased, the solubility of the solid bitumen under the UV light decreased, leaving partially dissolved and etched bitumen (Figure 13d-f). Some of this partially dissolved bitumen may still be soluble to organic solvent DCM depending on the type of bitumen (i.e. grahamite) macerals and thermal maturity (Jacob, 1989).

Chitinozoan and bitumen reflectance also increased with increasing pyrolysis temperatures. The measured chitinozoan reflectance of the Boas River Formation increased from 0.75 (original) to 0.87 and 1.39 %Ro_{chi} after 310 and 350 ^{o}C of pyrolysis, respectively (Figure 14). Using several most frequently used equations, the calculated VR_{eqv} from the measured chitinozoan indicates that these formations did indeed reach the oil window. The post-pyrolysis VR_{eqv} increased to 0.65 to 1.08 %Ro_{eqv} from the original 0.56 %Ro_{eqv} using the upper range of the Obermajer et al. (1996) conversion ratio (Ro_{chi} 20–25% higher than VR_{eqv}). Tricker et al. (1992) conversion equation [$VR_{eqv} = (R_{chi} - 0.08) / 1.152$] also produces similar results (0.68 to 1.1 %Ro_{eqv} from 0.58 %Ro_{eqv}) compared to those from the Obermajer et al. (1996) conversion ratio. Using the Bertrand (1990) equation ($Ro_{eqv} = 0.8873*Ro_{chi} + 0.0124$), the estimated Ro_{eqv} increased to 0.78 to 1.24 %Ro_{eqv} from 0.74%Ro_{eqv} after 310 and 350 ^{o}C of pyrolysis. This means that the Boas River Formation

already reached hydrocarbon generation (VR of 0.65-1.00 %Ro, Mukhopadhyay, 1994) before hydrous pyrolysis and it entered the thermogenic gas condensate window (VR >1.0 %Ro, Mukhopadhyay, 1994) after 350 ^{o}C of pyrolysis temperature.

The reflectance of the bitumen formed after the 310 and 350 ^{o}C pyrolysis are 0.57 and 1.15%Ro for the Boas River sample. These lead to an estimated VR_{eqv} of 0.75 and 1.08 $\%Ro_{eqv}$ using the Jacob (1989) equation (VR_{eqv} = 0.618 $\%Ro_{bit}$ + 0.40). The estimated VR_{eqv} using the Bertrand (1993) equation [Ro_{-evi} = 1.2503*$Ro_{-migrabitumen\ (limestones)}^{0.904}$] are 0.75 to 1.42 $\%Ro_{eqv}$. The Bertrand (1993) estimated Ro_{eqv} is significantly higher in comparison to the estimate from the Jacob (1989) equation at higher thermal maturity. The estimated Ro_{eqv} from Ro_{bit} (Bertrand, 1993) is also significantly higher than the estimated Ro_{eqv} from Ro_{bit} (Bertrand, 1990) at higher thermal maturity. The Tricker et al. (1992) and Obermajer et al. (1996) conversion ratios were also formulated from samples with similar paleodepositional environments to that of Bertrand (1993).

T_{max} Suppression

The results of organic solvent extraction show insignificant to minor differences (0 to 2 ^{o}C) between the T_{max} measured on the un-pyrolyzed extracted and unextracted samples (Tables 1 and 2), suggesting minimal T_{max} suppression for the onshore samples. This is consistent with T_{max} suppression observed by Snowdon (1995) in the Second White Speckled Shale from Alberta, Canada. Snowdon (1995) attributed the suppression of Tmax to the presence of extractable bitumen in the S2 peak and labile organic matter, which also coincides with high HI. Several authors have also suggested that Tmax suppression occurs due to elevated HI and presence of soluble bitumen in the rock matrix (Glikson et al., 1992; Stasiuk et al., 2005; and Hackley et al., 2013, Cardott et al., 2015).

In this study, Tmax suppression appeared to increase after the samples reach pyrolysis temperatures of 310 to 320 ^{o}C (Figure 6), which coincides with the highest volume of soluble organics (bitumen) and free hydrocarbons in the rock matrix (Figures 7 and 8). However, as the pyrolysis temperature increased the amount of soluble organics decreased, the Tmax suppression slightly declined or remained relatively the same (Tables 1, 2 and

Figure 6). This coincides with the increased in expulsion rate of hydrocarbon. On average, the Tmax values were suppressed by about 3 ^{o}C (range from 1 and 6 ^{o}C). The extent of Tmax suppression tends to be higher in the early stage of the hydrocarbon generation window (435-440 ^{o}C) (Figure 6). Tmax suppression can have a significant effect on determining the maturity level of some unconventional plays where the source rocks serve as reservoir, especially those in the peak hydrocarbon generation window. In such cases, solvent extraction is highly recommended to accurately determine the level of maturity when using RE analysis.

Expulsion Temperature and Rate

Small quantities of hydrocarbon where expelled after the 310 ^{o}C (T_{max} 431 to 437 °C) and 320 °C (Tmax 435 to 438 °C) pyrolysis temperatures for the Akpatok and Red Head Rapids formations, which generated 19.47 and 68.59 mg HC/ g TOC, respectively (Table 1). The subsequent pyrolysis temperature steps [330 °C (Tmax range of 438-440 °C) and 350 °C (Tmax range of 440-450 °C)] expelled much higher volumes of hydrocarbon, between 22.75 mg HC/g TOC and 166.22 mg HC/g TOC (Table 1). The increase in expulsion rate coincides with the increase in PI (Figure 11) which indicates that high volumes of volatile hydrocarbons (Figure 9) are present in the rock matrix (Table 1). The hydrocarbon saturation point and subsequent higher rate of expulsion was around pyrolysis temperatures of 320 to 330 ^{o}C or at T_{max} values of 435-440 ^{o}C, and peaked at around 340 and 350 ^{o}C (T_{max} of 442-450 ^{o}C). The variations in the amount of hydrocarbon (Table 1) expelled among these formations can be attributed to TOC content, compositional diversities of DOM and the porosity of the samples. Moreover, the differences in lithotypes and paleodepositional environments have a significant effect on the timing and chemical composition of the hydrocarbon generated (Stasiuk 1996; Stasiuk and Fowler, 2004; Peters et al., 2005a).

Transformation ratio of S2

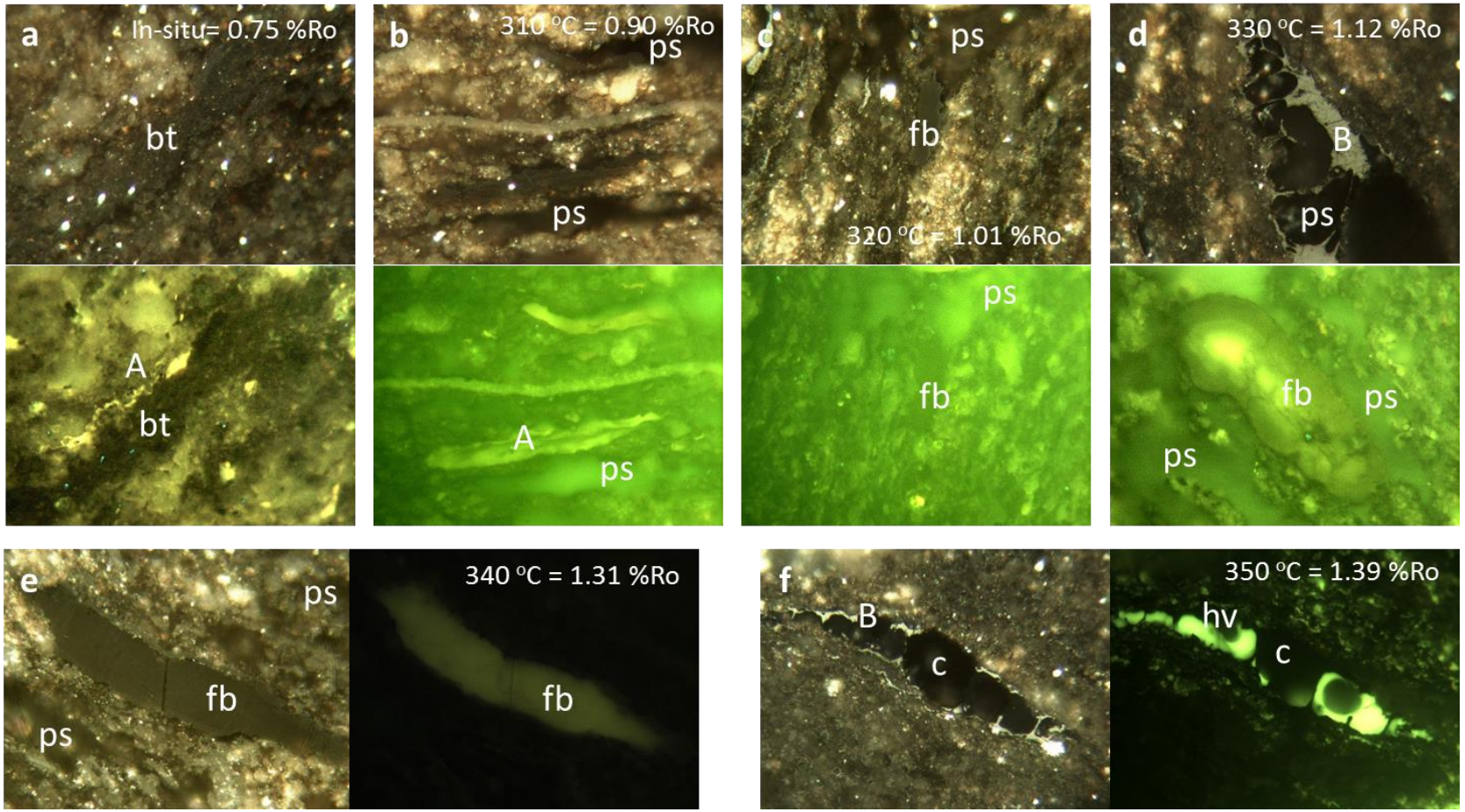

Figure 13. Photomicrographs of un-pyrolyzed (original) and pyrolyzed (310 to 350 °C) shale matrix from Boas River Formation with measured chitinozoan reflectance. a) Yellow fluorescing alginite (A) inclusion in bituminite (bt) matrix observed in as received samples. b-d) Greenish yellow surface stains, observed 310, 320, 320 °C pyrolysis temperature, are caused by residual hydrocarbon sorbed in the matrix. Pore spaces (ps) created by pyrolysis of bituminite, formation fluorescing soluble bitumen (fb) and non-fluorescing bitumen (B). e) Pore spaces vacated by bituminite macerals filled by fluorescing bitumen. f) Pore filling bitumen (B), bright fluorescing heavy oil (hv) and diagenetic carbonate (C). Reflected white and UV light in oil, 50 x magnifications. Image size 184 microns across.

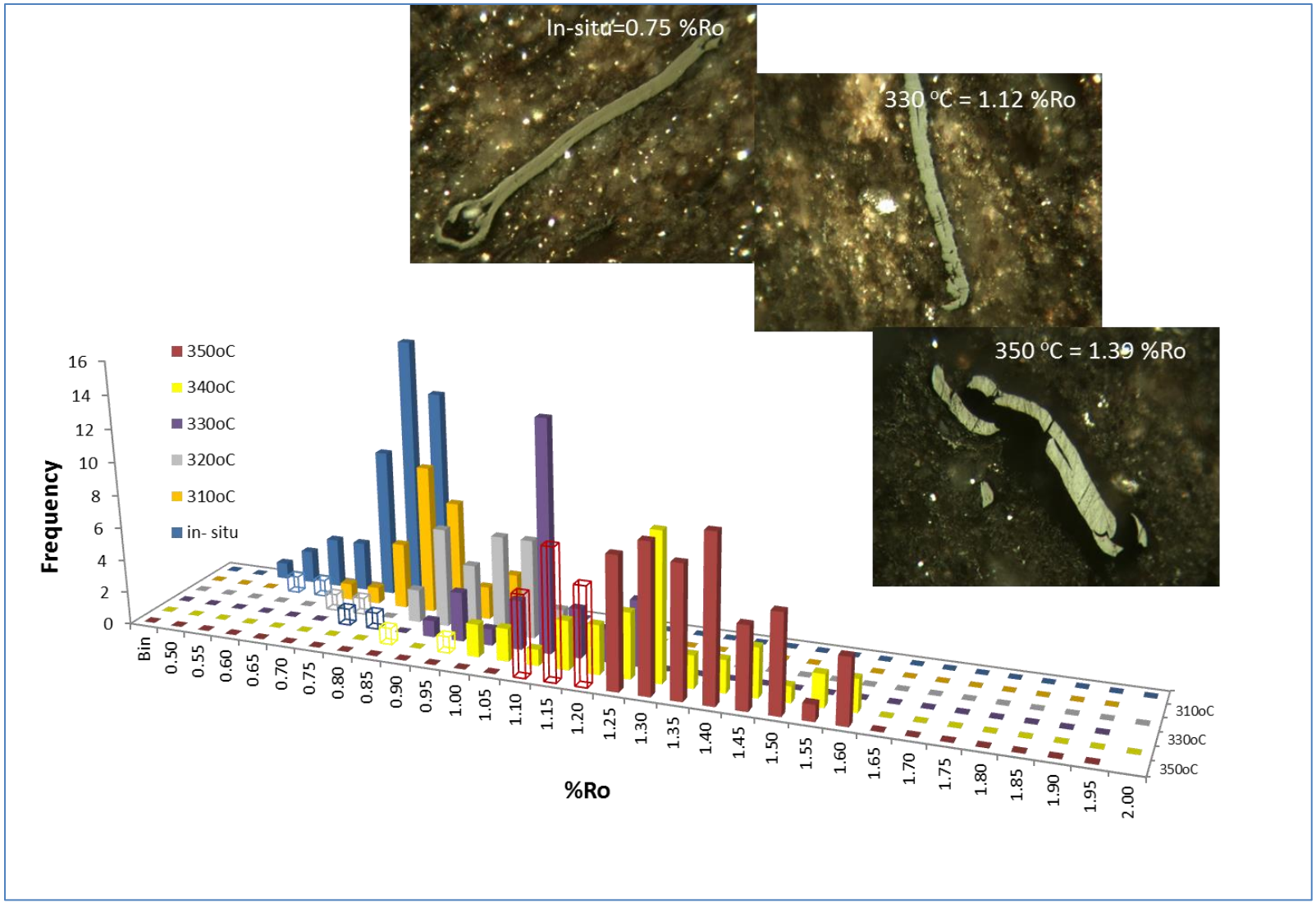

Figure 14. Measured chitinozoan (filled) and bitumen (unfilled) reflectance vs. pyrolysis temperature. Photomicrograph inserts showing chitinozoan macerals with average %Ro. Reflected white and UV light in oil, 50 x magnifications. Image size 184 microns across.

The thermal degradation of insoluble kerogen resulted in the transformation and generation of petroleum products (bitumen, oil, and gas) with increasing thermal maturity (Tissot and Welte, 1984; Lewan, 1985; Lafargue et al., 1998; Behar et al., 2001; McCarthy et al., 2011; Spigolon et al., 2015). The equation most commonly used to calculate transformation ratio of S2 is TR_{S2} (%) = ($S2_{original}$ − $S2_{residual}$)/($S2_{original}$)*100 (Tissot and Welte, 1984 and Bordenave et al. 1993, Spigolon et al., 2015). $S2_{original}$ is the original amount of insoluble reactive kerogen in the source rock. $S2_{residual}$ is defined as the residual petroleum generation potential of the source rock after hydrous pyrolysis. The TR_{S2} (%) is the amount of the $S2_{original}$ transformed into petroleum products. The calculated TR_{S2} range between 26 to 52% after 310°C pyrolysis temperature, with Boas River Formation having the highest TR (52%) compared to the other three formations (Table 1). The TR of S2 increased to 75 to 85% after the last pyrolysis temperature of 350°C.

Comparative analysis of the Rock-Eval data collected from the unextracted (p.unext) and extracted (p.ext) aliquots shows that the TR_{S2} values of the extracted samples ($S2_{p.ext}$, 47 to 92%) are higher than the TR_{S2} of the unextracted ($S2_{p.unext,}$ 26 to 85%) pyrolyzed samples (Tables 1 and 2). It seems that the presence of soluble organics is affecting not only the accurate determination of the T_{max} but also the transformation ratio. To determine the amount of soluble organic matter incorporated within S2 ($S2_{so}$), the following equation was used; $S2_{so} = S2_{p.unext} - S2_{p.ext}$, where $S2_{p.unext}$ is the measured S2 from unextracted pyrolyzed aliquots and $S2_{p.ext}$ is the S2 from the extracted pyrolyzed aliquots (Tables 1 and 2). The results show that approximately 31 to 52.42 % of the total $S2p._{unext}$ consists of extractable organic matter and only 47.58 to 69 % are insoluble kerogen. These extractable organics are derived from bitumen observed within fracture zones and pore spaces of the rock matrix (Figure 13c-d). Since the experiment is a closed system, the only possible sources of the bitumen are the hydrogen-rich reactive insoluble kerogen within the rocks matrix.

The results also show that the high amount of extractable organic matter in the rock matrix also leads to a significant overestimation of residual reactive kerogen/organic matter by 7 to 45% (calculated from Tables 1 and 2). The overestimation of S2 is more apparent during the early stage hydrous pyrolysis (310- to 330 ^{o}C), where the reactive kerogen thermally degraded into soluble bitumen (Figure 7) and as hydrocarbons formed within the rock matrix. The overestimation of residual S2 appears to decline exponentially as the bitumen thermally cracks into lighter oil, insoluble bitumen/pyrobitumen and gas during the latter stage of catagenesis (Jacob, 1989) and coincides with increased expulsion rate of

produce hydrocarbon. The overestimation of residual S2 will become negligible as the thermal maturity reaches the gas window (T_{max} >465, Peters and Cassa, 1994), where the remaining residual kerogen and insoluble bitumen thermally cracks into gas condensate, dry gas and pyrobitumen (Hunt, 1979; Tissot and Welte, 1984; Jacob, 1989; Hunt, 1996).

Statistical analyses reveal positive correlations between TR_{S2} and the measured T_{max} for both unextracted and extracted pyrolyzed samples (Figure 15). The strong positive linear correlations between $TR_{S2\ [p.unext\ and\ p.unext\ (+original)]}$ and T_{max} (Figure 15a) have almost identical R^2 (0.90 and 0.91, respectively) values (Note; the measured T_{max} of the original samples were included in the cross plot and in the calculation of R^2, since they are actual measurements and not predicted). In contrast, the positive correlations between the $TR_{S2\ [(p.ext\ and\ p.ext\ (+original)]}$ and T_{max} have dissimilar R^2 (0.84 and 0.91, respectively) values (Figure 15b). The extrapolated Y intercept of TR of $S2_{p.ext}$ is much higher than the estimated transformation ratio of $S2_{p.ext\ (+original)}$ based on the measured T_{max}. The relationship between Tmax and TR_{S2} is more curvilinear for the extracted samples if the data for the original unpyrolyzed samples are included in the analysis (Figure 15b, arrow).

Transformation ratio of HI

The equations most commonly used to calculate the transformation ratio of HI is TR_{HI} (%) = ($HI_{original} - HI_{residual}$) / $HI_{original}$)*100 (Bordenave et al., 1993). This equation uses the hydrogen index (HI) to estimate the residual petroleum generation potential of the source rocks instead of the S2. The calculated TR_{HI} of kerogen at 310 ^{o}C (T_{max} of 435 to 441 ^{o}C) to 350 ^{o}C (T_{max} of 451 to 455 ^{o}C) ranges from 16% to 67% for the Amadjuak Formation, 11% to 71% for the Akpatok Formation, 22% to 73% for the Red Head Rapid Formation, and 40% to 65% for the Boas River Formation (Table 1). Similar to the S2, the Boas River Formation has a higher HI transformation ratio at a lower pyrolysis temperature (310°C) compared to the other formations (40% versus 11 to 22%). The calculated TRs of the $HI_{p.ext}$ (22% to 82%; all four units) are significantly higher than the TRs of the $HI_{p.unext}$ aliquots

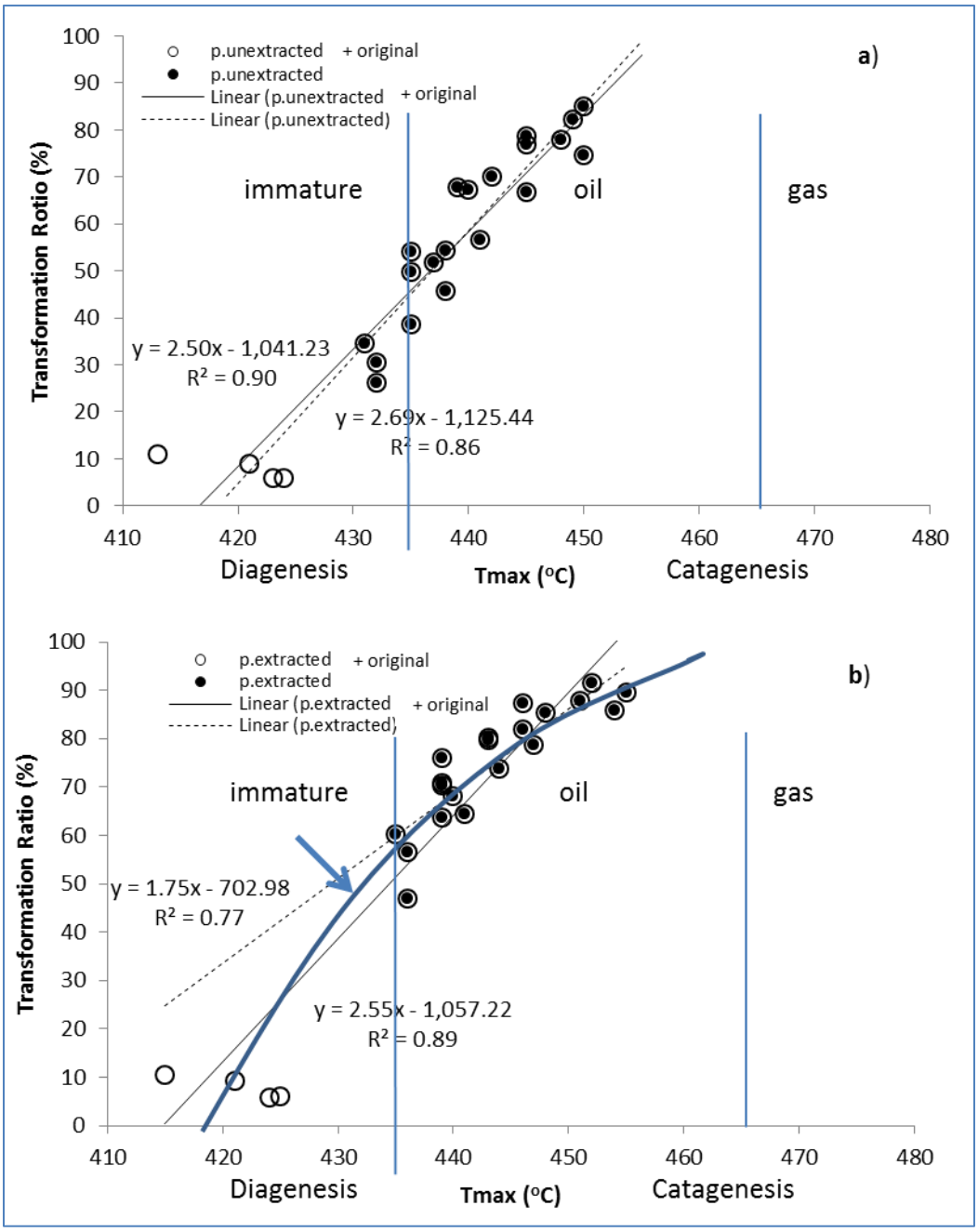

Figure 15. Transformation ratios derived from S2 as a function of T_{max}. a) Unextracted pyrolyzed rock chips. b) Extracted pyrolyzed rock chips.

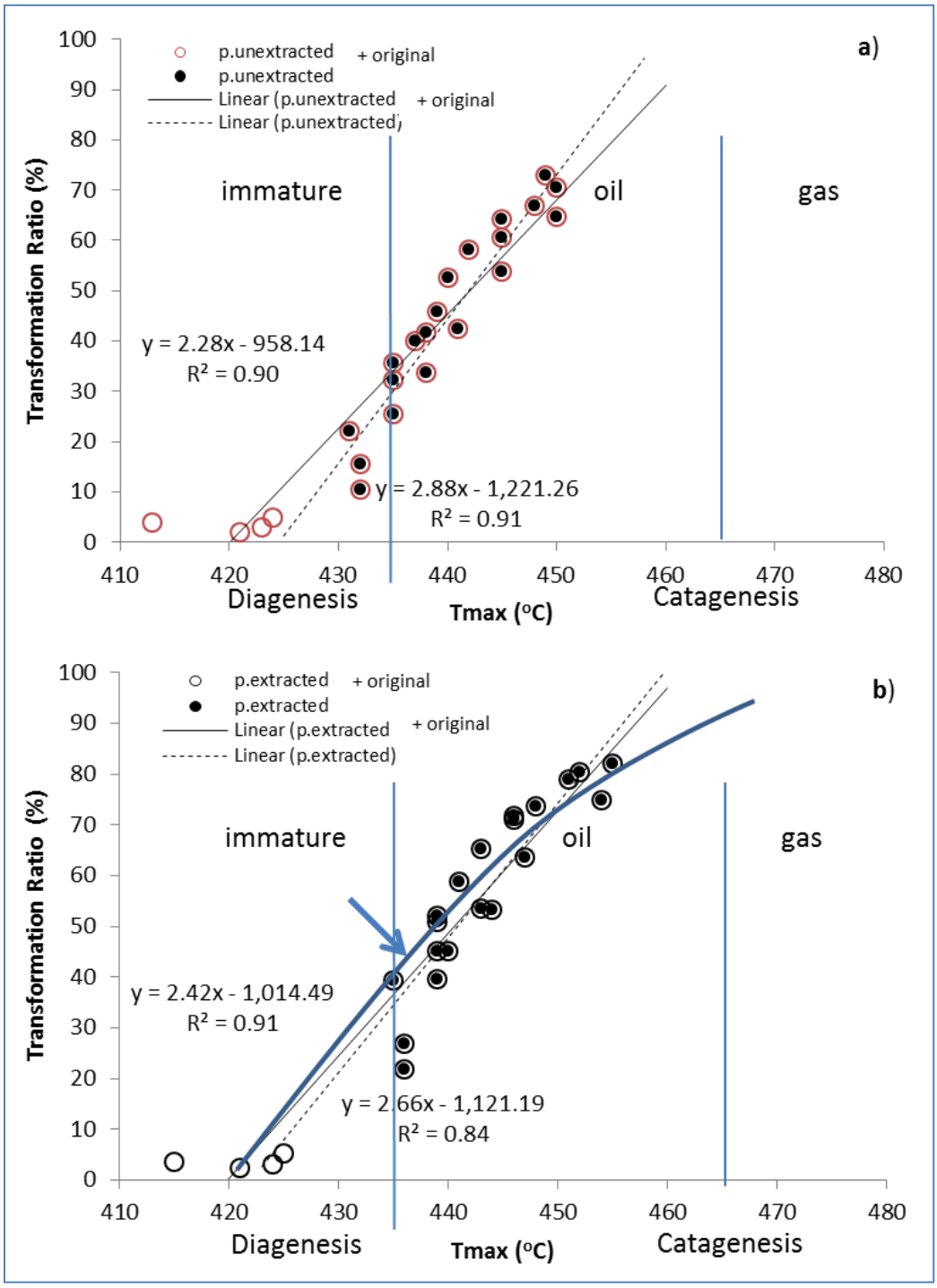

Figure 16. Transformation ratio based on HI as a function of T_{max}: a) Unextracted pyrolyzed rock chips; b) Extracted pyrolyzed rock chips.

(11% to 73%). The previously discussed overestimation of S2 has a significant impact on the calculated HI and the estimated TR, since they were calculated using S2 and TOC.

The transformation ratio of HI as a function of T_{max} also has strong positive correlations for both the unextracted and extracted samples (Figure 16a-b). However, the best fit curvilinear relationship between the TR of $HI_{p.ext}$ and T_{max} is slightly less than that for the TR of $S2_{p.ext}$ relationship (Figures 15b and 16b). These results are in agreement with the most recent observation by Waples and Tobey (2015) who also illustrated that the correlation between TR and HI is curvilinear rather than linear. They also stated that the underestimation of TR can have a significant impact on the accuracy of determining the total hydrocarbon generation potential of organic-rich mature source rock for unconventional plays. As discussed earlier, factors like lithology, mineralogy and organic facies may have an influence on the variation in TR of kerogen in concurrence with pyrolysis temperature.

Results Comparison and Basin Application

Previous Studies

Direct comparison between the results of this study and previous hydrous pyrolysis works by Lewan (1985), Hackley et al. (2013) and Spigolon et al. (2015) are not possible due to differences in methodology, age, kerogen type, and the paleodepositional environment of the samples. However, some general comparisons of the semi-quantitative and qualitative physicochemical parameters such the HCG and maturation pathways, peak bitumen and oil generation, and transformation ratio are possible. One of the most important parameters in distinguishing hydrocarbon generation and changes in thermal maturity is the formation and physicochemical evolution of bitumen during the latter stage of diagenesis and throughout catagenesis (Hunt, 1979; Lewan, 1985; Lewan, 1987; Jacob, 1989; Jacob, 1993; Hunt, 1996; Spigolon et al., 2015). In this study, the formation of void filling migrabitumen is a clear indicator that insoluble reactive kerogen has undergone thermal degradation. The appearance of bright, yellow fluorescing hydrocarbon inclusions in the matrix is also a good indicator of oil generation. However, it is important to determine whether the hydrocarbons were generated in-situ or whether they migrated into the rock from elsewhere. Pore-filling migrabitumen can also be observed far from source and into reservoir rocks and in highly porous stratigraphic layers along the migration

pathways (Lewan, 1987; Jacob, 1989; Jacob, 1993). The observed increase in reflectance and decrease in solubility of the bitumen viewed under UV light indicates that thermal maturity increases with increasing pyrolysis temperature, consistent with in situ hydrocarbon generation.

The bitumen reflectance increased to 0.60-1.15 %Ro from 0.50%$Ro_{original}$ after five levels of closed hydrous pyrolysis. These results are similar to work by Hackley et al. (2013), in which the reflectance of solid bitumen formed after hydrous pyrolysis increases to 0.45 to 1.3%Ro from 0.40 %$Ro_{original}$ after 300 to 360 ^{o}C pyrolysis experiments. The results of this study show that the HCG and maturation pathways are analogous to those of Hackley et al. (2013), even though the kerogen types (Cambrian-Ordovician to Eocene and Type I to Type III) are not identical.

Peak bitumen generation (soluble organics) and hydrocarbon expulsion were reached between 310-330 ^{o}C (T_{max} = 435-441 ^{o}C) and 340-350 ^{o}C (T_{max} = 440-455 ^{o}C), respectively (Table 1). Previous hydrous pyrolysis studies by Lewan (1985) and Spigolon et al. (2015) also documented similar peak bitumen [320-330 ^{o}C and 345-355 ^{o}C, and 310-330 ^{o}C (T_{max} = 430- 432 ^{o}C)] and oil generation [345 to 365 ^{o}C (T_{max} = 432- 437 ^{o}C)]. The dissimilarity between the measured T_{max} in our study and those of Spigolon et al. (2015) are likely due to differences in kerogen and mineralogical compositions and possible suppression, as they were measured using unextracted aliquots.

The calculated TR's of S2 (unextracted) after pyrolysis at 310 and 350 ^{o}C (26-52% and 75-85%, respectively) have slightly higher values at lower pyrolysis temperatures but are otherwise comparable to the results achieved by Spigolon et al. (2015) (20.3% and 77.8%, respectively). In comparison, the calculated TR's of S2 of the extracted aliquots are much higher than the results achieved by Spigolon et al. (2015) after 310 and 350 ^{o}C pyrolysis (47-65% and 86-92%, respectively). Similarly, the calculated TRs of HI after the 310 and 350 ^{o}C pyrolysis temperatures (11-42 % and 65-73%, unextracted) are also comparable to the calculated TR of HI values (22% and 67%) from the Spigolon et al. (2015) published data.

The variation in peak bitumen and oil generation, and TR among different samples is most likely due to the varying activation energies associated with the heterogeneous

character of the kerogen facies (Tissot and Welte, 1984). The thermal degradation of kerogen follows a fairly similar suite of first-order reactions with different activation energies that take place concurrently but independently of one another (Tissot and Welte, 1984). The different hydrogen content of various kerogen macerals and their corresponding activation energies play an important role in the TR of S2 and HI under similar thermal conditions. It is important to mention that the sample used by Spigolon et al. (2015) was Type I kerogen deposited in a lacustrine environment whereas samples used in this study were Type II kerogen deposited in a marine environment.

Basin Application

Geochemical data indicate that most of the Upper Ordovician formations are immature to early mature in the Hudson Bay and Foxe basins (T_{max} =410-435 °C) (Reyes et al., 2011, Bertrand and Malo, 2012, Lavoie et al., 2013). However, some younger organically lean stratigraphic layers have elevated T_{max}, both measured (>435 °C) and calculated ($T_{max-eqv}$ = 433-437°C), implying that some of organic-rich Upper Ordovician offshore formations have reached hydrocarbon generation (Bertrand and Malo, 2012; Lavoie et al., 2013). The large variation in T_{max} values between the organically-lean and organic-rich stratigraphic layers were partially attributed to T_{max} suppression (Lavoie et al., 2013). Although this study shows that T_{max} suppression was a factor for the unpyrolyzed as-received (0 to 2 ^{o}C) samples, the magnitude is much lower than the T_{max} suppression of 5 - 10 ^{o}C noted by Lavoie et al. (2013). Moreover, this observed variation in T_{max} is within analytical error and is therefore not significant with application to thermal maturity evaluation. As indicated earlier, T_{max} suppression increased substantially (1 to 6 ^{o}C) after the samples were artificially matured due to the increase in the amount of extractable organic matter in the S2 (Figure 7).

The detailed work on cuttings from the Polar Bear well (Zhang and Dewing, 2008; Zhang, 2008; Lavoie et al., 2013) suggests a T_{max} suppression between 5 - 10°C for the organic-rich Upper Ordovician Red Head Rapids Formation samples having TOC up to 2.3%; HI up to 465; T_{max} ranging between 418 to 448°C (average of 428°C, Lavoie et al., 2013; Annex 1.9). These RE results indicate that the Red Head Rapids Formation in the Polar Bear offshore well is more mature compared to its onshore equivalent. However, the observed large T_{max} variation cannot be attributed to T_{max} suppression associated with a high amount of soluble organic matter and labile hydrocarbons because most of the other RE

parameters are below the threshold values for in situ oil generation (PI = 0.1-0.4 and S1 >0.5, and S1:S2 <2.0 and S2:S3 ≥5.0, Peters and Cassa, 1994 and McCarthy et al., 2011). Furthermore, since the peak burial temperature (T_{max} 448°C) never went above the peak hydrocarbon generation window, these parameters would still show residual values indicating that hydrocarbon was generated in-situ even if migration has occurred. The RE values of the offshore Red Head Rapids Formation should be more or less comparable to the measured values in this study after hydrous pyrolysis.

It is more likely that the presence of labile bituminite (similar to that observed in Figure 13a) in the Red Head Rapids Formation is partly responsible for T_{max} suppression but not thermogenic bitumen and hydrocarbon generation. This would mean that the intra-stratigraphic T_{max} suppression is only between 0-2°C (original sample) and not 5-10°C, as suggested by Lavoie et al. (2013). Taking into consideration all the measured RE parameters, not just T_{max}, the offshore well (Beluga O-23, Narwhal South O-58, and Polar Bear C-11; Lavoie et al., 2013) data indicate that the Upper Ordovician stratigraphic layers have not yet reached the hydrocarbon generation stage. Obviously, detailed organic geochemistry and petrography would be needed for the offshore TOC-rich Upper Ordovician well cuttings to further confirm this interpretation.

Petrographically, some of estimated VR_{eqv} values suggest that these formations have reached early maturity (Reyes et al., 2011) and hydrocarbon generation (≥ 0.65 $\%Ro_{eqv}$) (Bertrand and Malo, 2012; Lavoie et al., 2013). However, none of these previously analyzed samples show any significant evidence of in-situ hydrocarbon generation. Instead, they contain amorphous bituminite which may have some associated labile and soluble organics as indicated by solvent extraction on the original samples. Likewise, the immature Upper Ordovician samples analyzed in this study do not show any signs of in-situ hydrocarbon generation (Figure 4). It was only after the first stage of pyrolysis (310 °C or T_{max} of ≥ 435) that significant amounts of fluorescing, soluble, migrated solid bitumen and free hydrocarbons were observed within intergranular pore spaces (Figure 13b-d).

The estimated VR_{eqv} from the measured T_{max} (0.67 to 1.03 $\%Ro_{eqv\text{-}ext}$), chitinozoan (0.68 to 1.1 $\%Ro_{eqv}$) and bitumen (0.75 to 1.08 $\%Ro_{eqv}$) reflectance indicates that all onshore source rock samples reach hydrocarbon generation only after the artificial maturation.

However, the Bertrand (1990 and 1993) equations indicate that all formations reach hydrocarbon generation (VR_{eqv} = 0.78 $\%Ro_{eqv\text{-}chi}$ and 0.75 $\%Ro_{eqv\text{-}bit}$) even before hydrous pyrolysis. These estimated VR_{eqv} values are much higher than the values obtained from the other equations referred to in this study with the exception of the Jacob (1989) equation. Moreover, these estimated VR_{eqv} values (1.24 $\%Ro_{eqv\text{-}chi}$ and 1.42 $\%Ro_{eqv\text{-}bit}$) are inconsistent with the physicochemical properties observed before hydrous pyrolysis and the changes that occurred after the artificial thermal degradation of kerogen (Figure 13). These results suggest that Bertrand's methodology may overestimate the vitrinite reflectance equivalent value and hence the thermal maturity.

Petrographic re-analysis of whole rock samples from the offshore Upper Ordovician source rocks from Beluga O-23, Narwhal South O-58, and Polar Bear C-11 could provide additional evidence which would indicate whether or not they reached hydrocarbon generation. The physicochemical evolution of kerogen observed in this study can be used as a template to determine if hydrocarbon generation and migration has occurred, particularly since most of the measured and estimated T_{max} data indicate that the samples are within the theoretical range of hydrocarbon generation (T_{max} = 430-465 °C, Lewan, 1993; Peters and Cassa, 1994; Lafargue et al., 1998; Behar et al., 2001; McCarthy et al., 2011; Spigolon et al., 2015). Soluble fluorescing bitumen would still be visible within the intergranular pore spaces of the rock matrix, if indeed these measured and estimated T_{max} values from offshore wells are an accurate measure of the maximum burial temperatures that resulted in hydrocarbon generation. Similarly, soluble and insoluble residual bitumen can also be observed within the intergranular pore spaces even after hydrocarbon migration has occurred.

The often contradictory geochemical data from the offshore wells [Beluga O-23, Narwhal South O-58, and Polar Bear C-11(Bertrand and Malo, 2012; Lavoie et al., 2013)] indicates that other factors may be responsible for the variation in thermal maturity indices. The most common source of error in Rock-Eval analysis is drilling contamination. Oil based mud and drilling additives are known to cause erroneous Rock-Eval data especially when using drill cuttings (Issler et al., 2016 and references therein). Additionally, severe recycling of higher maturity organic matter can create inconsistent high Rock-Eval T_{max} values. However, in-situ organic matter recycling maybe limited because of the age and

paleodepositional environment of these formations. Another possible source of the thermal maturity variation is the difference in the thermal conductivity of shale and limestones (Clark, 1966; Blackwell and Steele, 1989; Eppelbaum et al., 2014). The variation in mineral matrix in conjunction with the fast heating rate and high temperatures in laboratory simulation may also affect the rate of maturation and hydrocarbon generation (Yang and Horsfield, 2016). Further studies in these areas may be needed to determine what effect, if any, these factors have on thermal maturity of the these organic-rich formations. Unfortunately, such endeavors are currently outside the scope of this study.

CONCLUSIONS

This hydrous pyrolysis experiment generated source rock thermal maturation and hydrocarbon generation pathways that are comparable to the results of previous studies despite the various differences in equipment, methodology and samples. The measured and calculated organic geochemical parameters (HI, S1, S2, TOC, OI, PI, S2:S3, PC, and T_{max}) and the amount of expelled hydrocarbons indicate that these source rocks generated hydrocarbons during hydrous pyrolysis based on the source rock evaluation criteria of Peters and Cassa (1994) and McCarthy et al. (2011). The decrease in HI, S2, TOC, and S2:S3, and PC values and the simultaneous increase in S1, PI and T_{max} values indicate that all the source rocks were artificially matured through pyrolysis at 310 to 350°C for 72 hours.

Comparative analysis of the RE results before and after solvent extraction show that T_{max} suppression (1-6°C) arises due to a high amount of labile hydrocarbons and extractable organic matter such as soluble bitumen maceral asphaltite. The extent of T_{max} suppression in the as received samples is much lower (0-2 °C) than what was initially inferred (5-10°C) from previous studies. The high amount of solvent-extractable organic matter associated with S2 is also responsible for the overestimation of residual hydrocarbon generating potential and the underestimation of transformation ratio in the early stage of bitumen and hydrocarbon generation. T_{max} suppression, overestimation of S2 and underestimation of transformation ratio diminished as free hydrocarbons and soluble organic matter (bitumen) transform into light oil (mostly expelled), gas and pyrobitumen with increasing thermal maturity.

Peak bitumen formation and oil expulsion were reached at pyrolysis temperatures between 310-330 ^{o}C (T_{max} = 435-441 ^{o}C) and 340-350 ^{o}C (T_{max} = 440-455 ^{o}C), respectively, for the Upper Ordovician source rocks in this study. The volumes of oil expelled during peak hydrocarbon generation are between 56.93 mg HC/g TOC and 166.22 mg HC/g TOC after heating at pyrolysis temperatures of 340-350 ^{o}C. These peak oil generation and expulsion temperatures and the TR of HI and S2 are comparable to the results acquired in previous studies.

Organic petrography provided considerable morphological evidence for thermal degradation of reactive kerogen into bitumen, free hydrocarbons and residual insoluble solid bitumen. The estimated VR_{eqv} values from measured chitinozoan and bitumen reflectance, and the measured T_{max} all indicate that the studied samples reached the hydrocarbon

generation window after hydrous pyrolysis. Although the study was successful in simulating thermogenic hydrocarbon generation, it is important to note that this was still experimental and must be treated as such. Furthermore, while all the equations used in this study were useful substitutes for determining thermal maturity in the absence of direct thermal maturity measurements, the resulting VR_{eqv}, $T_{max\text{-}eqv}$, T_{max} and the Rock-Eval data as a whole must be carefully analyzed in conjunction with other available physicochemical information to make consistent and accurate interpretations.

ACKNOWLEDGEMENT

The authors would like to thank Patricia Webster and Krista Boyce of GSC-Calgary for processing samples and managing data; Richard Vandenberg of GSC-Calgary for the Rock-Eval Analysis. This manuscript benefited from Dr. Dale Issler comprehensive review and valuable inputs.

REFERENCES

ASTM, 2014. D7708-11 Standard test method for microscopical determination of the reflectance of vitrinite dispersed in sedimentary rocks. sec. 5, v. 05.06. In: Annual Book of ASTM Standards: Petroleum products, lubricants, and fossil fuels; gaseous fuels; coal and coke. ASTM International, West Conshohocken, PA, 10 pp.

Barker, C. E. and Pawlewicz, M.J. 1994. Calculation of vitrinite reflectance from thermal histories and peak temperatures In: P.K. Mukhopadhyay and W.G. Dow, Editors, ACS Symposium Series 570, Vitrinite reflectance as a maturity parameter, applications and limitations (1994), p. 216–229.

Behar, F., Vandenbroucke, M., Tang, Y., Marquis, F., Espitalié, J., 1997. Thermal cracking of kerogen in open and closed systems: determination of kinetic parameters and stoichiometric coefficients for oil and gas generation. Organic Geochemistry 26, p. 321–339.

Behar, F., Beaumont, V., Penteado H. L. De B., 2001. Rock-Eval 6 technology: performances and developments–Technologie Rock-Eval 6: performances et développements. Oil & Gas Science and Technology - Rev. IFP. 56, 2, p. 111–134.

Bertrand, R. 1990. Correlations among the reflectance of vitrinite, chitinozoans, graptolites and scolecodonts. Organic Geochemistry 15, p. 565–574.

Bertrand, R. 1993. Standardization of solid bitumen reflectance to vitrinite in some Paleozoic sequences of Canada. Energy Sources Journal 15, p. 269–288.

Bertrand, R., and M. Malo, 2012, Dispersed organic matter reflectance and thermal maturation in four hydrocarbon exploration wells in the Hudson Bay Basin: regional implications: Geological Survey of Canada, Open File 7066, 54 pp.

Blackwell, D.D. and Steele, J.L., 1989. Thermal conductivity of sedimentary rocks: measurement and significance. In: Naeser ND, McCulloch TH (Ed.) Thermal history of sedimentary basins. Springer, New York, p 5–96.

Bordenave, M.L., Espitalié, J., LePlat, P., Oudin, J.L., Vandenbroucke, M., 1993. Screening techniques for source rock evaluation. In: Bordenave, M.L. (Ed.), Applied Petroleum Geochemistry. Editions Technip, Paris, p. 217–278.

Cardott, B.J., C.R. Landis, and M.E. Curtis, 2015, Post-oil solid bitumen network in the Woodford Shale, USA—A potential primary migration pathway: International Journal of Coal Geology, 139, p. 106–113.

Clark, S.P. Jr 1966. In: Clark, S.P. Jr (Ed.), Handbook of physical constants (revised edition), Geological Society of America. Memoir 97, Washington, DC.

Curiale, J.A., 1986. Origin of solid bitumens, with emphasis on biological marker results Organic Geochemistry 10, p. 559-580.

Decker, V., P. Budkewitsch, and W. Tang, 2013. Reconnaissance mapping of suspect oil seep occurrences in Hudson Bay and Foxe Basin using satellite radar: Geological Survey of Canada, Open File 7070, 19 pp.

Diessel, C.F.K. & Bailey, J.G. (1989). The application of petrographic techniques to carbonisation and combustion research at the University of Newcastle. – MINPET 89, p. 117–121.

Eggie, L.A., Pietrus, E., Ramdoyal, A. and Chow, N. 2014. Diagenesis of the Lower Silurian Ekwan River and Attawapiskat formations, Hudson Bay Lowland, northern Manitoba (parts of NTS 54B, F, G); in Report of Activities 2014, Manitoba Mineral Resources, Manitoba Geological Survey, p. 161–171.

Eppelbaum, L., Kutasov, I. and Pilchin, A., 2014. Thermal properties of rocks and density of fluids, Lecture notes in earth system sciences, in Applied Geothermics, DOI: 10.1007/978-3-642-34023-9_2, Springer-Verlag Berlin Heidelberg.

Espitalie, J., Madec, M. and Tissot, B. Role of mineral matrix in kerogen pyrolysis: Influence on petroleum generation and migration. American Association Petroleum Geologists Bulletin 64, 1, p. 59−66.

Espitalié, J., Deroo, G. and Marquis, F. (1985a) La pyrolyse Rock-Eval et ses applications. Oil & Gas Science and Technology, 40, 5, p. 563-579.

Espitalié, J., Deroo, G. and Marquis, F. (1985b) La pyrolyse Rock-Eval et ses applications. Oil & Gas Science and Technology, 40, 6, p. 755-783.

Espitalié, J., Deroo, G. and Marquis, F. (1985c) La pyrolyse Rock-Eval et ses applications. Oil & Gas Science and Technology, 41, 1, p. 73-89.

Glikson, M., Taylor, D., and Morris, D., 1992. Lower Paleozoic and Precambrian petroleum source rocks and the coalification path of alginite. Organic Geochemistry 18, p. 881–897.

Goodarzi, F., Reyes, J., Schulz, J., Hollman, D., Rose, D. 2006. Parameters influencing the variation in mercury emissions from an Alberta power plant burning high inertinite coal over thirty-eight week's period. International Journal of Coal Geology 26, p. 26–34.

Hackley, P.C., Bove, A.M., Dulong, F.T., Lewan, M.D., Valentine, B.J., 2013. Reevaluation of vitrinite reflectance suppression through hydrous pyrolysis experiments. Abstract. 65th Annual Meeting of the International Committee for Coal and Organic Petrology. August 25-31, 2013, Sosnowiec, Poland. p. 32.

Hackley, P.C. and Cardott, B.J. 2016. Application of organic petrography in North American shale petroleum systems: A review. International Journal of Coal Geology 163, p. 8–51.

Hunt, J. M., 1979. Petroleum geochemistry and geology: W. H. Freeman, San Francisco,

California, 617 p.

Hunt, J. M., 1996. Petroleum geochemistry and geology, 2nd Edition: W. H. Freeman, San Francisco, California, 743 p.

Heywood, W.W., and B.V. Sanford, 1976. Geology of Southampton, Coats, and Mansel Islands, District of Keewatin, Northwest Territories: Geological Survey of Canada, Memoir 382, 35 p.

International Committee for Coal Petrology, (ICCP), 1993. International handbook of coal petrography, 3rd Supplement to 2nd Edition. University of Newcastle on Tyne (England).

Issler, D., Reyes, J., Chen, Z., Hu, K., Negulic, E., Grist, A., Stasiuk, L., Goodarzi, F., 2012 Thermal history analysis of the Beaufort-Mackenzie Basin, Arctic Canada. In, Proceedings of the 32nd Annual GCSSEPM Foundation Bob F. Perkins Research Conference; Rosen, N C (ed.); Weimer, P (ed.); Coutes dos Anjos, S M (ed.); Henrickson, S (ed.); Marques, E (ed.); Mayall, M (ed.); Fillon, R (ed.); D'Agostino, T (ed.); Saller, A (ed.); Campion, K (ed.); Huang, T (ed.); Sarg, R (ed.); Schroeder, F (ed.); p. 609-641; 1 DVD

Issler, D.R., Jiang, C., Reyes, J., and Obermajer, M., 2016. Integrated analysis of vitrinite reflectance, Rock-Eval 6, gas chromatography, and gas chromatography-mass spectrometry data for the Reindeer D-27 and Tununuk K-10 wells, Beaufort-Mackenzie Basin, northern Canada; Geological Survey of Canada, Open File 8047, 94 p. doi:10.4095/297905

Institut français du Pétrole, 1987. IFF kinetics, in MATOIL program version 1.2 manual: Bureau d'Études Industrielles et de Coopération de 1'Institut français du Pétrole, appendix C.

Jacob, H., 1989. Classification, structure, genesis and practical importance of natural solid oil bitumen ("migrabitumen"). International Journal of Coal geology 11, p. 65–79.

Jacob, H., 1993. Nomenclature, Classification, Characterization, and Genesis of Natural Solid Bitumen (Migrabitumen). In: Parnell, J., Kucha, H., Landais, P., (Eds.). Bitumens in ore deposits. Special Publication of the Society for Geology Applied to Mineral Deposits 9. Springer-Verlag, p. 11–27.

Jarvie, D.M., 1991. Factors affecting Rock-Eval derived kinetic parameters. Chemical Geology 93, p. 79–99.

Jarvie, D. M., and L. L. Lundell, 2001. Amount, type, and kinetics of thermal transformation of organic matter in the Miocene Monterey Formation, in C. M. Isaacs and J. Rullkotter, eds., The Monterey Formation: From rocks to molecules: New York, Columbia University Press, chapter 15, p. 268–295.

Jenkins, W. A. M, 1970. Chitinozoa. Proceedings of the First Annual Meeting, October 1968. Geoscience and Man, Vol. 1. American Association of Stratigraphic Palynologists 1, pp. 1-21.

Lafargue, E., Marquis, F., and Pillot, D., 1998. Rock-Eval 6 applications in hydrocarbon exploration, production, and soil contamination studies. Revue de l'Institut Français du Pétrole 53, p. 421– 437.

Landis, C.R., Castaño, J.R., 1995. Maturation and bulk chemical properties of a suite of solid hydrocarbons. Organic Geochemistry 22, p. 137–149.

Lavoie, D., Pinet, N., Dietrich, J., Zhang, S., Hu, K., Chen, Z., Asselin, E., Galloway, J., Decker, V., Budkewitsch, P., Armstrong, D., Nicolas, J. Reyes, M., Brake, V., Duchesne, M.J., Kohn, B.P., Keating, P., Craven, J., and Roberts, B., 2013. Geological framework, basin evolution, hydrocarbon system data and conceptual hydrocarbon plays for the Hudson Bay and Foxe basins, Canadian Arctic: Geological Survey of Canada, Open File 7363, 200 p.

Lavoie, D., Pinet, N., Dietrich, J., and Chen, Z., 2015. The Paleozoic Hudson Bay Basin in northern Canada: new insights into hydrocarbon potential of a frontier intracratonic basin. American Association Petroleum Geologists Bulletin 99, p. 859-888.

Lewan, M.D., 1985. Evaluation of petroleum generation by hydrous pyrolysis experimentation. Philosophical Transactions of the Royal Society of London A315, p. 123–134.

Lewan, M.D., 1987. Petrographic study of primary petroleum migration in the Woodford Shale and related rock units. In: Doligez, B. (Ed.), Migration of Hydrocarbons in Sedimentary Basins. Editions Technip, Paris, p. 113–130.

Lewan, M.D., 1993. Laboratory simulation of petroleum formation: Hydrous pyrolysis, in Engel, M., and Macko, S., eds., Organic Geochemistry, Plenum Publications Corp., New York, p. 419–442.

Lewan, M.D., 1997. Experiments on the role of water in petroleum formation. Geochimica et Cosmochimica Acta 61, 3691–3723.

Lewan, M.D., Winters, J.C., McDonald, J.H., 1979. Generation of oil-like pyrolyzates from organic-rich shales. Science 203, p. 897–899.

Lewan, M.D., Ruble, T.E., 2002. Comparison of petroleum generation kinetics by isothermal hydrous and non-isothermal open-system pyrolysis. Organic Geochemistry 33, 1457–1475.

Lewan, M.D., Roy, S., 2011. Role of water in hydrocarbon generation from Type-I kerogen in Mahogany oil shale of the Green River Formation. Organic Geochemistry 42, 31–41.

Lipps, J. H. (ed.) 1993. Fossil prokaryotes and protists. Boston, Oxford, London, Edinburgh, Melbourne, Paris, Berlin, Vienna: Blackwell Scientific. 342 pp.

Macauley, G., 1987, Geochemistry of organic-rich Ordovician sediments on Akpatok and Baffin Islands, Northwest Territories: Geological Survey of Canada, Open File 1502, 27 pp.

Macauley, G., M.G. Fowler, F. Goodarzi, L.R. Snowdon, and L.D. Stasiuk, 1990,

Ordovician oil shale — source rock sediments in the central and eastern Canada mainland and eastern Arctic areas, and their significance for frontier exploration: Geological Survey of Canada, Paper 90–14.

Mackowsky, M.-Th. 1982. Methods and tools of examination. In E. Stach, M.-Th. Mackowsky M. Teichmuller, G.H. Taylor, D. Chandra, and R. Teichmuller (eds.), Stach's Textbook of coal Petrology, 3rd ed., Berlin: Gerbruder Borntaeger, p. 295–299.

McCarthy, K., Rojas, K., Niemann, M., Palmowsky, D., Peters, K., Stankiewicz, A., 2011. Basic petroleum geochemistry for source rock evaluation. Oilfield Review 23, no. 2. p. 32–43.

Moldowan, J. M., Lee, C. Y., Sundararaman, P., Salvatori, T., Alajbeg, A., Gjukic, B., Demaison, G. J., Slougue, N. E. and Watt, D. S., 1992. Source correlation and maturity assessment of select oils and rocks from the central Adriatic Basin (Italy and Yugoslavia), in J. M. Moldowan, P. Albrecht, and R. P. Philp, eds., Biological markers in sediments and petroleum: Englewood Cliffs, New Jersey, Prentice-Hall, 411 p.

Mukhopadhyay, P. K., 1994. Vitrinite reflectance as maturity parameter: Petrographic and molecular characterization and its applications to basin modeling. Vitrinite reflectance as a maturity parameter, applications and limitations. Edited by and W. G. Dow; American Chemical Society Symposium Series 570; American Chemical Society: Washington, DC, 1994; 294 pp.

Noble, R.A., Wu, C.H., Atkinson, C.D., 1991. Petroleum generation and migration from Talang Akar coals and shales offshore N.W. Java, Indonesia. Organic Geochemistry 17, p. 363–374.

Obermajer, M., Fowler, M.G., Goodarzi, F., Snowdon, L.R., 1996. Assessing thermal maturity of Palaeozoic rocks from reflectance of chitinozoa as constrained by geochemical indicators: an example from southern Ontario, Canada. Marine Petroleum Geology, 13, p. 907–919.

Pepper, A.S., and Corvit, P.J., 1994. Simple kinetic models of petroleum formation. Part I: oil and gas generation from kerogen. Marine and Petroleum Geology 12, 3, p. 291–319.

Peters, K. E., 1986, Guidelines for evaluating petroleum source rocks using programmed pyrolysis: American Association Petroleum Geologists Bulletin 70, p. 318–329.

Peters, K.E., Moldowan, J.M., and Sundararama, P., 1990. Effects of hydrous pyrolysis on biomarker thermal maturity parameters: Monterey Phosphatic and Siliceous members. Organic Geochemistry 15, 3, p. 249–265.

Peters, K.E., Walters, C.C., and Moldowan, J.M., 2005a. The biomarker guide, Volume 1: Biomarkers and Isotopes in the Environment and Human History: Prentice Hall, Inc. Cambridge, U.K., 471 pp.

Peters, K.E., and Cassa, M.R., 1994, Applied source rock geochemistry, in Peters et al., 2005. Magoon, L.B., and Dow, W.G., eds., The petroleum system—From source to trap: Tulsa, Okla., American Association of Petroleum Geologists Memoir 60, p. 93–117.

Peters, K.E., Walters, C.C., and Moldowan, J.M., 2005b. The Biomarker Guide, Volume 2: Biomarkers and Isotopes in Petroleum Exploration and Earth History: Cambridge, U.K., 1157 pp.

Petersen, H.I., Bojesen-Koefoed, J.A., Nytoft, H.P., 2002. Source rock evaluation of Middle Jurassic coals, northeast Greenland, by artificial maturation: aspects of petroleum generation from coal. American Association of Petroleum Geologists Bulletin 86, p. 233–256.

Petersen, H.I., Nytoft, H. P., Nielsen, A.T., 2004. Characterisation of oil and potential source rocks in the northeastern Song Hong Basin, Vietnam: indications of a lacustrine-coal sourced petroleum system. Organic Geochemistry 35, p. 493–515.

Petersen, H.I., Schovsbo, N.H., Nielsen, A.T., 2013. Reflectance measurements of zooclasts and solid bitumen in Lower Paleozoic shales, southern Scandinavia: correlation to vitrinite reflectance. International Journal of Coal Geology 114, p. 1–18.

Pinet, N., D. Lavoie, J. Dietrich, K. Hu, and P. Keating, 2013a. Architecture and subsidence history of the Hudson Bay intracratonic basin: Earth Science Reviews 125, p. 1–23.

Pinet, N., Keating, P., Lavoie, D., 2013b. Did the Hudson Strait in Arctic Canada record the opening of the Labrador Sea? Marine and Petroleum Geology 48, p. 354-365.

Potter, J., Stasiuk, L.D., Cameron, A.R. (Eds.), 1998. A petrographic atlas of Canadian coal macerals and dispersed organic matter (Canadian Society for Coal Science and Organic Petrology). 105 pp.

Reyes, J., Goodarzi, F., Sanei, H., Stasiuk, L.D., Duncan, W., 2006. Petrographic and geochemical characteristics of organic matter associated with stream sediments in Trail area British Columbia, Canada. International Journal of Coal Geology 26, p. 146–157.

Reyes, J., D. Armstrong, and D. Lavoie, 2011, Organic petrology of James Bay Basin. Ontario Petroleum Institute, 50th Annual meeting.

Reyes, J., McMechan, M.E., and Ferri, F., 2015a. Vitrinite reflectance data for selected samples from Devono-Mississippian and Lower Cretaceous shale cores in the Liard Basin area, northeast British Columbia; Geological Survey of Canada, Open File 7902, 1 .zip file. doi:10.4095/297164

Reyes, J., Lane, L., Moignard, P. Mort, A., 2015b. Petrographic analyses of the thermal discontinuity at the Canol and Ogilvie Formation boundary of N. Parkin D-61 well from Eagle Plain, Yukon, Canada. 67th Annual Meeting of the International Committee for Coal and Organic Petrology. September 5-11, 2015, Potsdam, Germany. p. 138-140.

Snowdon, L.R., 1995. Rock-Eval T_{max} suppression: documentation and amelioration. American Association Petroleum Geologists Bulletin 79, p. 1337–1348.

Spigolon, A.L.D., Lewan, M.D., Penteado, L.H.B., Coutinho, F.C., Mendonça Filho, J.G., 2015. Evaluation of the petroleum composition and quality with increasing thermal maturity as simulated by hydrous pyrolysis: A case study using a Brazilian source rock with Type I kerogen. Organic Geochemistry 83-84, p. 27–53.

Stach, E., Mackowsky, M.-Th., Teichmuller, M., Taylor, G.H., Chandra, D., Teichmuller, R., 1982. Stachs Textbook of Coal Petrology, 3rd ed. Gebrüder Borntraeger, Berlin. 535 p.

Stasiuk, L.D., 1993. Algal bloom episodes and the formation of bituminite and micrinite in hydrocarbon source rocks: evidence from the Devonian and Mississippian, northern Williston Basin, Canada. International Journal of Coal Geology 24, 195-210.

Stasiuk, L.D., 1996. Microscopic studies of sedimentary organic matter: Key to understanding organic-rich strata, with Paleozoic examples from Western Canada Basin. Geoscience Canada 26, 4, p. 149-172.

Stasiuk, L.D. and Fowler, M.G. 2004. Organic facies in Devonian and Mississippian strata of Western Canada Sedimentary Basin: relation to kerogen type, paleoenvironment, and paleogeography. Bulletin of Canadian Petroleum Geology 52, 3, p. 234-255.

Stasiuk, L.D., Goodarzi, F., Bagheri-Sadeghi, H., 2005. Petrology, rank and evidence for petroleum generation, Upper Triassic to Middle Jurassic coals, Central Alborz Region, Northern Iran. International Journal of Coal Geology 67, p. 249–258.

Seifert, W.K. and Moldovan, J.M., 1980. The effect of thermal stress on source-rock quality as measured by hopane stereochemistry. In: J.R. Maxwell, Editor, *Physics and Chemistry of the Earth*, Pergamon, Oxford (1980), p. 229–237.

Soldan, A.L., Santos Neto, E.V., Cerqueira, J.R., Concha, F.J.M., Branco, V.A.C., Arai, M., 1988. Hydrous-pyrolysis: a tool to access maturation. Boletim de Geociências da Petrobras 2, 65–76.

Souza, I.V.A.F., Araújo, C.V., Menezes, T.R., Coutinho, L.F.C., Binotto, R., Spigolon, A.L.D., Fontes, R.A., Santos Neto, E.V., Rondon, N.D.V.F., Mendonça Filho, J.G., 2014. Organic and mineral matter changes due to oil generation, saturation and expulsion process based on artificial maturation experiments. Geologica Acta 12, p. 351–362.

Taylor, G.H., Liu, S.Y. and TeichmiJller, M., 1991. Bituminite-- a TEM view. International Journal of Coal Geology 18, p. 1269-1273.

Teichmüller, M., 1974. Generation of petroleum-like substances in coal seams as seen under the microscope. In: B. Tissot and F. Bienner (Editors), Advances in Organic Geochemistry, 1973. Editions Technip, Paris, pp. 379-405.

Teichmüller, M. (1987a): Recent advances in coalification studies and their applications to geology. – In: Scott, A.C. (Ed.): Coal and Coal-Bearing Strata: Recent Advances, Geol. Soc. Spec. Publ., Blackwell Sci. Publ., Oxford, 32, 127-170

Tegelaar, E.W., Noble, R.A., 1994. Kinetics of hydrocarbon generation as a function of the molecular structure of kerogen as revealed by pyrolysis-gas chromatography. Organic Geochemistry 22, p. 543–574.

Tissot, B.P., Welte, D.H., 1984. Petroleum formation and occurrence, second ed. Springer-Verlag, Berlin.

Tissot, B.P., Pelet, R., Ungerer, Ph., 1987. Thermal history of sedimentary basins, maturation indices, and kinetics of oil and gas generation. American Association of Petroleum Geologists Bulletin 71, p. 1445–1466.

Tricker, P. M., Marshall, J.E.A. and Badman, T.D. 1992. Chitinozoan reflectance: a Lower Paleozoic thermal maturity indicator. Marine and Petroleum Geology 9, p. 302-307.

Tyson, R.V., 1995. Sedimentary organic matter. Chapman & Hall, London. Utah Geologic Survey, 2014, Cumulative oil production reported for Duchesne and Uintah counties, Utah. <http://oilgas.ogm.utah.gov/pub/Publications/Reports/Prod/County/Cty_Oct_2014.pdf>.

Waples, D. and Tobey, M. H., 2015 Like Space and Time, Transformation Ratio is Curved. Search and Discovery Article #41713 (2015) Posted October 26, 2015.

Winters, J.C., Williams, J.A., Lewan, M.D., 1983. A laboratory study of petroleum generation by hydrous pyrolysis. In: Bjorøy, M. (Ed.), Advances in Organic Geochemistry 1981. John Wiley & Sons, New York, pp. 24–533.

Yang, S. and Horsfield, B., 2016. Some predicted effects of minerals on the generation of petroleum in nature. Energy Fuels 30, p. 6677−6687.

Zhang, S., 2008. New insights into Ordovician oil shales in Hudson Bay Basin: their number, stratigraphic position, and petroleum potential: Bulletin of Canadian Petroleum Geology 56, p. 300–324. doi:10.2113/gscpgbull.56.4.300

Zhang, S. 2011, Geochemistry data from three oil shale intervals in unit 1, Red Head Rapids Formation (Upper Ordovician) on Southampton Island: Geological Survey of Canada, Open File 6681, 23 p. doi:10.4095/288109.

Zhang, S. 2012. Ordovician stratigraphy and oil shale, southern Baffin Island, Nunavut–preliminary field and post-field data; Geological Survey of Canada, Open File 7199, 26 p.

Zhang, S., and K. Dewing, 2008, Rock-Eval data for four hydrocarbon exploration wells in Hudson Bay and Foxe basins: Geological Survey of Canada, Open File 5872, 25 p. doi:10.4095/225633.